

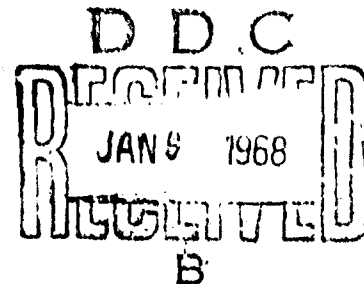
1022

AD 663423

A STUDY OF THREE-DIMENSIONAL, INCOMPRESSIBLE,
TURBULENT WALL JETS

by

Pasquale M. Sforza and Gary Herbst



OCTOBER 1967

POLYTECHNIC INSTITUTE OF BROOKLYN

DEPARTMENT
of
AEROSPACE ENGINEERING
and
APPLIED MECHANICS

PIBAL REPORT NO. 1022

Distribution of this document is unlimited.

AFOSR 67-2580

A STUDY OF THREE-DIMENSIONAL, INCOMPRESSIBLE,
TURBULENT WALL JETS

by

Pasquale M. Sforza and Gary Herbst

Research sponsored by Air Force Office of
Scientific Research, Office of Aerospace
Research, United States Air Force. Research
monitored under the technical supervision of
Major Donald L. Calvert, AFOSR.

Polytechnic Institute of Brooklyn

Department

of

Aerospace Engineering and Applied Mechanics

October 1967

PIBAL Report No. 1022

A STUDY OF THREE-DIMENSIONAL, INCOMPRESSIBLE,
TURBULENT WALL JETS[†]

by

Pasquale M. Sforza* and Gary Herbst**

Polytechnic Institute of Brooklyn

SUMMARY

This report presents an experimental investigation of the mean properties of turbulent, three-dimensional, incompressible air jets issuing into a quiescent air ambient from various rectangular orifices parallel to, and at the surface of, a flat plate. An analytical approach to estimate the shear stress distribution at the plate is also presented.

The flow field of a three-dimensional wall jet is found to be characterized by three distinct regions in the axis velocity decay. From the results obtained it is concluded that for three-dimensional wall jets the maximum velocity in the flow in the near field exhibits a decay rate dependent on orifice geometry, while far downstream of the jet exit it decays at the same rate as that in a radial wall jet flow field independent of orifice geometry. Furthermore, it is shown that the growth of the mixing layer normal to the plate is apparently independent of orifice shape while the near field spanwise growth is affected by initial geometry.

[†] This research was supported by the Air Force Office of Scientific Research under Contract No. AF 49(638)-1623, Project No. 9781-01.

* Assistant Professor of Aerospace Engineering.

** NSF Graduate Trainee

Irregularities in the spanwise distribution of streamwise mean velocity attest to the strong three-dimensionality in the near field of the wall jets studied. These irregularities are manifested as local excesses, or defects, in the velocity profile. Such results indicate that the characterization of the wall jet flow field generated by a finite slot as quasi-two-dimensional may be of questionable validity.

TABLE OF CONTENTS

<u>Section</u>		<u>Page</u>
I	Introduction	1
II	Experimental Apparatus	4
III	Presentation and Discussion of Results	7
IV	Concluding Remarks	28
V	References	30

LIST OF ILLUSTRATIONS

<u>Figure</u>		<u>Page</u>
1	Schematic Representation of Flow Field of Three- Dimensional Wall Jet	35
2	Wall Jet Test Facility	36
3	End Cap Schematic.	37
4	Static Pressure Distribution ($e=.10$)	38
5	Details of Probe Design.	39
6	View of Framework for Adjustment of Wall Flatness in Wall Jet Facility	40
7	Maximum Velocity Decay for $e=.025$	41
8	Maximum Velocity Decay for $e=.05$	42
9	Maximum Velocity Decay for $e=.10$	43
10	Maximum Velocity Decay for $e=1.0$	44
11	Maximum Velocity Decay for $e=10$	45
12	Half Width Growth for $e=.025$	46
13	Half Width Growth for $e=.05$	47
14	Half Width Growth for $e=.10$	48
15	Half Width Growth for $e=1.0$	49
16	Composite of $Y_{1/2}$ for All Wall Jets Tested	50
17	Composite of $Z_{1/2}$ for All Wall Jets Tested	51
18	Half Width Growth for $e=10$	52

LIST OF ILLUSTRATIONS (Contd)

<u>Figure</u>		<u>Page</u>
19	Axial Velocity Profiles in Characteristic Decay Region	53
20	Axial Velocity Profiles in Radial Type Decay Region. .	54
21	Axial Velocity Profiles in Characteristic Decay Region	55
22	Axial Velocity Profiles in Radial Type Decay Region. .	56
23	Axial Velocity Profiles in Characteristic Decay Region	57
24	Axial Velocity Profiles in Radial Type Decay Region. .	58
25	Axial Velocity Profiles in Radial Type Decay Region. .	59
26	Axial Velocity Profiles in Radial Type Decay Region. .	60
27	Axial Velocity Profiles in Radial Type Decay Region. .	61
28	Axial Velocity Profiles in Radial Type Decay Region. .	62
29	Transverse Velocity Profiles	63
30	Transverse Velocity Profiles	64
31	Transverse Velocity Profiles	65
32	Transverse Velocity Profiles	66
33	Transverse Velocity Profiles	67
34	Transverse Velocity Profiles (d=.10") for e=.10 Slot .	68
35	Transverse Velocity Profiles (d=.10") for e=.10 Slot .	69
36	Transverse Velocity Profiles (d=.07") for e=.05 Slot .	70
37	Transverse Velocity Profiles (d=.05") for e=.025 Slot.	71

LIST OF ILLUSTRATIONS (Contd)

<u>Figure</u>		<u>Page</u>
38	Contours of Constant Velocity for $e=0.10$ Slot	72
39	Comparison of Maximum Velocity Decay for Free Jet and Wall Jet.	73
40	Exponent (N) of Maximum Velocity Decay for Free Jets and Wall Jets Within CD Region.	74
41	Comparison of Free Jet and Wall Jet for $e=0.10$	75
42	Comparison of Mean Velocity Profiles Between Wall Jet and Free Jet Emanating From Same ($e=0.10$) Orifice, $x=1.0$ inch	76
43	Comparison of Mean Velocity Profiles Between Wall Jet and Free Jet Emanating From Same ($e=0.10$) Orifice, $x=2.0$ inch	77
44	Surface Flow Studies	
	a. $e=0.025$	78
	b. $e=0.05$	78
	c. $e=0.10$	79
	d. $e=1.0$	79
	e. $e=10.0$	80
45	Side (a) and Top (b) View of $e=0.05$ Flow Field.	81
46	Side (a) and Top (b) View of $e=1.0$ Flow Field	82
47	Three-Quarter View of $e=0.10$ Flow Field	83

LIST OF SYMBOLS

CD	Characteristic Decay
C_f	skin friction coefficient, Eq. (14)
d	height of orifice
e	eccentricity of orifice, d/l
l	length of orifice
PC	Potential Core
RD	Radial-type Decay
Re	Reynolds number
u	mean velocity in X-direction
v,w	mean transverse velocity components
X	streamwise coordinate
Y	spanwise coordinate
Z	normal coordinate
ζ	transformed normal coordinate, $Z/Z_{1/2}$
η	transformed spanwise coordinate, $Y/Y_{1/2}$
θ	Eq. (7)
ν	kinematic viscosity
ρ	density
τ	shear stress
τ_{XY}	axial shear stress on planes normal to Y-axis
τ_{XZ}	axial shear stress on planes normal to Z-axis

Subscripts

m,max denotes conditions at maximum velocity point

LIST OF SYMBOLS (Contd)

- w denotes conditions at the wall
- X,Y,Z denotes differentiation with respect to the indicated variable
- o denotes conditions along the X-axis
- $\frac{1}{2}$ denotes conditions at $u/u_m = \frac{1}{2}$
- 2-D denotes two-dimensional flow conditions

Superscripts

- $\bar{(\)}$ denotes $(\)/d$ unless otherwise specified

I. INTRODUCTION

An experimental investigation of the mean properties of turbulent, three-dimensional, incompressible jets of air issuing into a quiescent air ambient, tangent to, and at the surface of, a rigid flat plate is presented. A schematic diagram of the flow field appears in Fig. 1. Herein such flows are termed "three-dimensional wall jets." An exploratory investigation of such a three-dimensional flow field was presented by Viets and Sforza¹. Their results are extended in this report.

Experimental investigations of "two-dimensional" as well as radial wall jets have been performed by Sigalla², Bakke³, Bradshaw and Gee⁴, Poreh et al.⁵, among others⁶⁻¹¹. A very useful annotated bibliography on wall jets has been prepared by Rajaratnam and Subramanya¹².

Sigalla's² primary objective was the determination of the surface skin friction distribution in a so-called "two-dimensional" wall jet whereas Bakke's³ study centered upon a comparison of his experimental observations with Glauert's theoretical predictions for a radial wall jet. Bradshaw and Gee⁴ extensively explored both mean and turbulent properties of "two-dimensional" wall jets and presented measurements of mean velocity and turbulence intensity profiles, skin friction coefficients, etc. A similar investigation of radial wall jets has been performed by Poreh et al.⁵

In the present investigation the flow fields were generated by a rectangular orifice. Each orifice possessed a different eccentricity,

here defined as the ratio of the height to the length of the orifice, but all orifices were of equal area. Hence, all the flows were observed under conditions of equal initial momentum flux.

It was found that all conventional three-dimensional wall jets, i.e., those whose orifice eccentricity is less than or equal to unity, may be characterized by three distinct regions in terms of the axial decay of the maximum velocity as suggested by Viets and Sforza¹. This feature is analogous to that encountered in the description of three-dimensional free jets as demonstrated by Sforza et al.¹³ Furthermore, irregularities in the spanwise distribution of the mean streamwise velocity for the conventional three-dimensional wall jets have been observed, similar to the mean velocity irregularities in three-dimensional free jets reported by Trentacoste and Sforza¹⁴. These irregularities in the mean velocity profile, manifested as local excesses and defects, pose a difficulty in specifying what region of a wall jet flow field generated by a long, slender slot is even quasi-two-dimensional. Hence the use of the quotation marks about the term two-dimensional in the previous discussion. The implications of these features of wall jet flow field will be discussed subsequently.

Finally, an estimate of the streamwise variation of the skin friction coefficient for three-dimensional wall jets is presented. The results of the analysis, which is based on an integral form of the conventional boundary layer equations, indicate that the streamwise variation of the skin friction coefficient is independent of the

spanwise growth of the mixing layer and is a function of the ratio of the characteristic dimension of the mixing layer (the half-width) normal to the plate to the streamwise coordinate, X . The major assumption utilized in the derivation is that the spanwise surface shear stress is similar; this result is shown to be reasonable, particularly in the far field of the wall jet.

II. EXPERIMENTAL APPARATUS

A. Wall Jet Facility

Photographs of the wall jet facility are presented in Fig. 2. A 5 hp. compressor maintains a minimum pressure of 120 pounds in a 19 cubic foot storage tank. Immediately after leaving the tank the air is dried and filtered. Further downstream in the supply line the pressure is controlled by two manual loading pressure regulators in series. Controlled low pressure air then enters the 8 3/4-inch diameter, 21-inch long settling chamber from the 1/2-inch diameter supply line. In the chamber the incoming flow passes through a double baffle of perforated metal provided to damp out pressure surges and to further decelerate the flow. A typical end cap for the settling chamber is shown in Fig. 3. Each cap has an orifice of different eccentricity but an equivalent area of $.100 \pm .002$ sq. in. The end cap to orifice area ratio is 260. The surface of the cap is machine finished and the bolt holes for securing the end cap are blind so as to afford a smooth unbroken surface. No leaks were detected at the junction of the settling chamber and the end plates.

The settling chamber is mounted on a rigid support which can be adjusted in the three coordinate planes. The highly polished 4x6 ft. aluminum plate is also adjustable for precise alignment with the settling chamber and the steel channel section beneath the plate carrying the traversing probe unit. The latter can also be adjusted and locked in any of the three coordinate directions. With it, measurements

can be accurately taken within .005 inches in the Z and Y directions.

B. Pressure Sensing System

The total head and static pressure measurements were obtained by utilizing vertical manometers with water as the manometer fluid. Pressure differentials of 0.05 inches of water were easily read with this system.

For the total head measurements, the vertical manometer allows a range of more than 50 inches of water. In the case of the static pressure measurements in the flow, however, where small variations occur, the manometer was used in an inclined position. A typical static pressure profile normal to the plate is shown in Fig. 4 for a particular orifice and X-station and is similar to that presented in Ref. 17. The pressure does not return to exactly ambient pressure far from the plate due to wetting of the manometer tube surface. The measured values of static pressure were not used in the calculation of the mean velocity since the observed effect was found to be so small that the tedium involved in amassing the necessary data was unwarranted in the present study.

The two probes used in the present investigation are shown in Fig. 5. Both probes are of standard design; no attempt was made to evaluate the different static probe designs considered by some to be essential to static pressure measurements in turbulent flows. This was another reason for neglecting static pressure variation in computing the mean velocity. A disadvantage of the probes utilized is the slow

time response, especially in the bleed mode. On the average, readings were taken every five minutes.

The total head and static pressure probes were mounted on a manually operated carriage. This carriage rested upon an accurately machined hexagonal bar, supported by an inverted steel channel. As mentioned previously, the plate was also adjustable, as shown in Fig. 6. The entire assembly was painstakingly aligned.

The settling chamber pressure was continuously monitored to avoid fluctuations greater than ± 0.2 inches of water. Readings were taken only when the chamber pressure was within this limit. All tests were performed with an exit velocity of 208 fps.

C. Flow Visualization

For the surface flow visualization studies, the plate was sprayed with a lampblack and kerosene solution; the flow was then initiated and continued until the flow pattern was fully visible. By this method it was possible to study the spread of the jet over the surface of the plate. Unfortunately this technique could not be used to show the spread of the jet normal to the plate. Therefore, photographic studies of a modelled wall jet flow field in the PIBAL water tunnel were performed in order to indicate more completely the gross features of the turbulent mixing process under investigation. The photographs obtained in this study will be discussed subsequently.

III. PRESENTATION AND DISCUSSION OF RESULTS

A. General Features

It has been shown by Viets and Sforza¹ that three distinct regions may be defined for a three-dimensional wall jet (refer to Fig. 1). These regions are described by the different rates of decay of the maximum velocity along the centerline of the jet, and may be classified as follows:

(1) Potential Core (PC) Region: Here the flow is characterized by a constant maximum velocity which is equal, or very close to, the jet exit velocity.

(2) Characteristic Decay (CD) Region: In this second region the maximum velocity decays as a constant power of X (streamwise distance) and indicates that the mixing from the near boundaries (the top side of the orifice and the flat plate) of the jet has reached the center of the flow region, but the mixing from the far boundaries (the sides) has not yet permeated the entire flow field. Therefore, in this region orifice end effects are important; hence the axis decay of mean velocity is termed characteristic of the particular orifice considered.

(3) Radial Type (RD) Decay Region: Finally, the mixing from all the boundaries of the jet has permeated the entire flow field. The maximum velocity decays like that of a radial wall jet, i.e., an axisymmetric jet which impinges normally upon a

wall and spreads radially over the wall. In this region the flow becomes increasingly oblivious of the orifice geometry. The division of the flow field into these regions may be more clearly visualized by referring to the schematic diagram in Fig. 1.

B. Maximum Velocity Decay

Of primary concern in studies of the present type is the decay of the maximum mean velocity with X , the streamwise coordinate. In general, for a situation in which the flow field could be properly termed two-dimensional or radially symmetric, the maximum mean velocity in a profile taken normal to the plate in any purely streamwise direction is well-defined. However, as was stated earlier, the maximum mean velocity in a three-dimensional wall jet does not occur necessarily on the symmetry axis (here the X -axis) in the CD region. This is the phenomenon described as velocity "irregularities" introduced, for the wall jet flow fields, by Viets and Sforza¹. This feature of three-dimensional wall jets will be discussed at greater length in a subsequent section of this report. For the moment it is only necessary to state that in the present report the term mean maximum velocity denotes the maximum mean velocity in a profile taken normal to the plate along the X axis in the plane $Y=0$.

Quite an extensive amount of work has been performed on turbulent incompressible wall jets, as can be seen in the annotated bibliography compiled by Rajaratnam and Subramanya¹².

In the case of "two-dimensional" wall jets, the decay of maximum velocity has been reported by Sigalla² and Bradshaw and Gee⁴ to be roughly proportional to $X^{-0.5}$. However, the results of the present investigation indicate that the definition of a two-dimensional region within the flow field generated by a finite slot may be quite arbitrary. Indeed, it is not clear, in view of the velocity irregularities observed in the transverse profiles, what relationship exists between the results obtained from slot jets and the truly two-dimensional counterpart. Sigalla², among others, noted similar irregularities in his data which, he found, could not be attributed to experimental error.

It will be shown, subsequently, that long, narrow orifices ($e \ll 1$) generate flow fields which have highly irregular mean velocity profiles in the transverse direction, within the CD region. It has been suggested that this phenomenon is closely related to the vortex structure of the wall jet flow field by Viets and Sforza¹. A detailed investigation of the nature of these mean flow nonuniformities is presented by Sforza and Trentacc¹⁵.

In close agreement with other experiments, Bakke³ found that for a radial wall jet the maximum velocity decay is $X^{-1.12 \pm 0.03}$. This agrees quite well with the maximum velocity decay in the RD region for the "slender" ($e \ll 1$) and the "bluff" ($e = O(1)$) orifices as determined by the present study.

For the "slender" orifices of eccentricity $e=0.025$ and $e=0.05$ the maximum velocity in the CD region decays as $X^{-.41}$ and $X^{-.44}$, respectively. These results are in fair agreement with those of Sigalla² and Bradshaw and Gee⁴. In the RD region $U_m \sim X^{-1.15}$ for both orifices, indicating a radial type wall jet decay as found by Bakke³. The results for these cases are shown in Figs. 7 and 8.

Viets and Sforza¹ have shown that for a three-dimensional wall jet with an orifice of eccentricity $e=0.10$, the maximum velocity decays as $X^{-0.162}$ and $X^{-1.144}$ for the CD region and RD region, respectively. It was thought that perhaps the plate used in that experiment was too small and thus generated adverse effects due to flow "spillage" off the sides. For this reason the complete flow field was re-investigated using the more refined apparatus described previously. The maximum velocity decay is shown in Fig. 9 and is found to be proportional to $X^{-0.16}$ in the CD region and $X^{-1.09}$ in the RD region. These results agree quite well with the preliminary results of Ref. 1. Again the decay in the RD region is equal to that found for the radial wall jet.

For the square orifice ($e=1.0$), there is a direct transition to a radial wall jet decay. This is shown in Fig. 10, where the maximum velocity is seen to decay as $X^{-1.14}$.

The flow field for the $e=1.0$ orifice (i.e., the $e=0.10$ orifice with its narrow side tangent to the plate) was investigated primarily out of curiosity since it fits neither the "slender" nor the "bluff"

orifice description. As seen from Fig. 11, the maximum velocity decay is proportional to $X^{-.76}$ and is neither so-called two-dimensional nor radial in behavior. It will be shown that near the exit the flow is essentially that of a three-dimensional free jet emanating from the same orifice.

C. Velocity Half-Widths

Two velocity half-widths appear in the present problem: one normal to the plate ($Z_{1/2}$), the other parallel to it ($Y_{1/2}$). The former, the normal half-width, is the largest distance between the plate and the point in the profile (normal to the plate) where the mean velocity is one-half its maximum value in that profile. Similarly, the transverse half-width ($Y_{1/2}$) is the distance between the $Y=0$ plane and the point in the profile (parallel to the plate) at which the mean velocity is one-half its maximum value in that profile.

Figs. 12 and 13 present the transverse half-width growths for the $e=0.025$ and $e=0.05$ orifice. Here it is seen that $Y_{1/2}$ is a constant in the near region of the flow field and then begins to increase as the flow develops further.

For the orifices $e=0.10$ and $e=1.0$, a different type of pattern is observed. Figs. 14 and 15 show that for both orifices $Y_{1/2}$ first decreases, crosses over $Z_{1/2}$, and then rapidly increases. Here, the transverse half-width is said to "neck-down" in the CD region.

From Figs. 16 and 17, which are composites of the half-width growths for the "slender" and "bluff" orifices, two important

conclusions can be deduced. First, the $Z_{\frac{1}{2}}$ (normal half-width) growths in the X-direction are essentially the same for all the conventional wall jets tested. Secondly, far downstream the $Y_{\frac{1}{2}}$ (transverse half-width) growth becomes oblivious of the orifice geometry, since again the growth rate becomes identical for all the flows. It may be noted here that the normal and transverse growth rates are not equal; the spreading across the plate is the more rapid far downstream.

For the $e=10.0$ orifice, the two half-widths are presented in Fig. 18. Note the sharp $Y_{\frac{1}{2}}$ growth, indicating a rapid transverse spreading of the jet as it flows along the plate. Within the range of streamwise distance studied, it is apparent that there is little change in the growth normal to the plate.

D. Similarity of Velocity Profiles

For each one of the wall jets tested the flow region was investigated for flow similarity. Glauert¹⁶ has obtained theoretical descriptions for wall jets for cases in which similarity exists for both two-dimensional and radial wall jets. Here, for the three-dimensional wall jet flows investigated, similarity was observed in both the CD and RD regions. These results have been compared with Glauert's predictions.

Figs. 19 through 24 present centerline similarity profiles normal to the plate for the $e=0.025$, $e=0.05$, and $e=0.10$ orifices. In the characteristic decay regions these profiles agree quite well with Glauert's two-dimensional profiles ($\alpha=1.25$). Those in the radial decay

region are in very good agreement with his results for the radial wall jet profile ($\alpha=1.3$). It must be noted that the differences in the profiles described by the two different values of α are not great.

Figs. 25 and 26 present the normal velocity similarity profiles for the $e=1.0$ and $e=10.0$ orifices, respectively. Here again both compare well with Galuert's similarity velocity profile for a radial wall jet, even though the maximum velocity decay is not that of a radial wall jet in the case of the $e=10.0$ orifice. The latter result implies that the half-width growth is quite a powerful factor in ensuring flow similarity.

An extensive study was performed on the $e=0.10$ orifice wall jet to determine whether or not profile similarity exists off the $Y=0$ plane. Figs. 27 and 28 present such normal (X,Z plane) similarity profiles for the RD region. These indicate that normal profile similarity exists up to $\bar{Y}=2.0$ off the centerline, but ceases at $\bar{Y}=2.5$.

Similarity profiles in the transverse direction for the RD region are also presented for all the orifices in Figs. 29 through 33. All of these profiles were taken at a height $Z=Z_m$ off the plate except for Fig. 31. In Fig. 31, profiles for the $e=0.10$ orifice at an arbitrarily picked height of $Z=0.06$ inches from the plate are depicted. For all the orifices except $e=10.0$ the similarity profiles are approximately the same.

E. Velocity Irregularities

Nonuniformities in the velocity distribution in planes parallel to the plate have been reported by a number of investigators studying the flow field of "so-called" two-dimensional wall jets. In most cases, only brief mention is made of these irregularities, e.g., Sigalla², Schwarz and Cosart⁷, Bradshaw and Gee⁴, Kruka and Eskinazi⁸; by others, such as Nishimura¹⁸, data has been presented, and in Viets and Sforza¹ data is presented and an explanation is offered.

Here, as shown for the three-dimensional free jet by Sforza, Steiger, and Trentacoste¹³, and Trentacoste and Sforza¹⁴, the velocity irregularities appear in the near field (CD region). In the three-dimensional free jet the velocity irregularities are believed to be caused by the induced velocity distribution connected with a system of vortex rings surrounding the jet.

The wall jet flow field is generally considered to be split into two parts as one proceeds in a direction normal to the plate. That is, an inner portion which exhibits the characteristics of a boundary layer flow over a flat plate and an outer portion which exhibits the characteristics of a free jet type flow field. It is believed that a system of vortex rings surrounds this outer portion of the flow field, as in the case of the free jet, and induces velocities which give rise to this irregular behavior in the velocity distribution parallel to the plate. As the flow proceeds downstream in X, these vortex rings merge and diffuse (as in the case of the free jet), thus reducing the

effectiveness of their induced velocity field.

Far downstream in the RD region, no trace of this irregular behavior in the velocity distribution parallel to the plate can be observed, thus indicating that complete diffusion of the surrounding vortex rings has taken place. A more complete description of this phenomenon has been given by Sforza and Trentacoste¹⁵.

Some representative results of these irregularities from the present investigation for the $e=0.10$ orifice at different heights above the plate are presented in Fig. 34. They are present at $X=2$ in. but cease to exist at $X=3$ in. as is shown in Fig. 35. Results for the orifices $e=0.05$ and $e=0.025$ are presented in Figs. 36 and 37, respectively. These transverse velocity profiles were taken at the height where the velocity in the profile normal to the plate was a maximum. Here again, as for the $e=0.10$ orifice, the velocity irregularities decay with the streamwise coordinate X .

F. Extent of Two-Coordinate Flow

For the more slender jets tested, i.e., $e=0.025$ and 0.05 , there appears to be a region of two-coordinate flow. That is, the irregularities are no longer discernible and a relatively flat velocity profile in the spanwise direction is observed, as in Figs. 36 and 37. Furthermore, this occurs within the CD region of the jet. One would be tempted to suggest that this restricted region of the flow field is quasi-two-dimensional. There are three objections to this conclusion:

- (1) The magnitude of the nonuniformities generally increases

as Z increases beyond Z_{\max} . A maximum is achieved and then the magnitude of the velocity irregularities decreases as Z is increased further. Therefore, there may exist irregularities in the flow field at $Z > Z_{\max}$ even though there is a small extent of uniform velocity in the spanwise direction at $Z = Z_{\max}$.

(2) The contours of constant velocity, as shown in Fig. 38, indicate that the flow field is somewhat oval in cross-section. Therefore, the spanwise extent of uniform flow is quite small near the plate, increases as Z increases, and then diminishes as Z increases beyond Z_{\max} . In turn, the spanwise extent of two-coordinate flow throughout the full profiles normal to the plate is much smaller than indicated by the flat portion of the velocity profiles at the Z_{\max} station.

(3) Finally, and most importantly, the stations at which this uniformity of maximum velocity across a small portion of the flow field in the Y -direction appears is immediately preceded by the region of large velocity nonuniformities. This phenomenon has been suggested to be due to the presence of a strong, concentrated vortex superstructure, and its attendant induced velocity field, by Sforza and Trentacoste¹⁵. Therefore, it appears that the vortex structure, which is dependent upon the orifice geometry and is highly three-dimensional in character, has strongly influenced the flow field prior to its attaining a small measure of uniformity.

This indicates that the concentrated vorticity has been effectively dissipated by turbulent mixing and the more regular profile is a result of this dissipation. The resulting smooth profile is achieved by turbulent diffusion and its subsequent decay is diffusive in character, i.e., smooth, with a "rounding-out" of the profiles.

The conclusion that may be drawn from the above is that in certain cases a small region wherein the flow is spanwise-uniform about the X-axis may be isolated. However, it appears that there is no reason to assume that this flow is connected to its two-dimensional counterpart since its previous history is strongly dependent on the three-dimensional vortex superstructure of the flow.

G. Isovels

For each X-station the maximum velocity, determined from the normal centerline velocity profile, was used to nondimensionalize the velocity field at that station. For the orifice of $e=0.10$, contours of constant u/u_{\max} at $X=3, 5, \text{ and } 7$ inches are presented in Fig. 38. From these contours the streamwise development of the flow field and the influence of the wall is readily apparent.

H. Comparison of Wall and Free Jets

Three-dimensional wall jets have many features in common with those of their free jet counterparts. Both flow fields may be conveniently divided into three distinct regions based on the streamwise decay of the maximum velocity. Each region in the wall jet flow field is

analogous to its free jet counterpart:

- (1) Both have potential core regions.
- (2) Both have characteristic decay regions in which the orifice geometry has an important effect.
- (3) Both have an asymptotic decay region where the effects of orifice geometry become unimportant and where the flow behaves as if it were generated by a point source. For the wall jet this region is termed the radial decay region wherein the flow field is in many ways similar to that of a radial wall jet. In the case of the free jet the asymptotic region is termed the axisymmetric decay region because the flow field approaches axisymmetry in its entirety.

Indeed, the maximum velocity decay for both free jets and wall jets are very similar in appearance as shown in Fig. 39. In both cases the maximum velocity distribution in the CD region is clearly dependent on the orifice geometry. However, as the flow proceeds further downstream, all the decay rates approach the appropriate asymptotic value: $u_m \sim X^{-1}$ and $X^{-1.1}$ for the free jets and wall jets, respectively. It is interesting to note that the dissipation due to wall shear is less effective than that due to free shear in retarding the maximum velocity. For example, at $X=10$ in., the maximum velocity in the wall jet is roughly 10% to 20% greater than that of the free jet.

Further evidence of the similarities between wall jets and free jets, with respect to the streamwise decay of maximum mean velocity,

is depicted in Fig. 40. Here the exponent n , which describes the decay of maximum velocity according to the relation $u_m \sim X^{-n}$, is plotted for various values of e for both wall jets and free jets within the CD region. It is evident that the variation of n for increasing e is not monotonic for both types of flow fields.

Trentacoste and Sforza¹⁴ found that the free jet with $e=0.10$ had superior mass entrainment properties compared to the axisymmetric jet; the former also displayed the "slowest" decay rate of maximum velocity. Other investigations^{19,20} indicate that optimum mass entrainment is achieved by free jets with $0.083 < e < 0.125$; the $e=0.10$ jet falls in this range. It may develop that a similar result will transpire for the wall jet flow field, i.e., that wall jets generated by orifices with an eccentricity $e \approx 0.10$ have optimum mass entrainment characteristics. Clearly, this would be of great importance in connection with slot-jet injection systems.

It appears then that the effect of the wall on maximum velocity decay is not very pronounced. However, its influence on the streamwise growth of the wall jet is appreciable and readily apparent. In the case of the free jet, Trentacoste and Sforza¹⁴ observed that free jets generated by "slender" orifices possess similar half-width growths. That is, all half-width data in both principal planes may be reduced to a single plot for all regions of the flow by utilizing a growth parameter based on the eccentricity of the orifice.

In the case of the wall jet it has been shown in Fig. 17 that the half-width growth normal to the plate ($Z_{1/2}$) is practically equivalent for all conventional orifices tested. A perusal of Fig. 16 shows that in the CD region the $e=0.025$ and 0.05 jets have transverse half-width growths ($Y_{1/2}$) which are monotonic, while those in the $e=0.10$ and 1.0 jets are not monotonic. The similarities between these growths for the free jets and wall jet is closest in the case of the $e=0.10$ orifice as shown in Fig. 41. It is clear that the presence of the wall inhibits the "necking-down" of the more slender wall jets which had been observed in the free jet flow fields¹⁴.

Far downstream all the wall jets spread transversely at about the same rate. It may be pointed out that this spreading occurs at a faster rate than in the free jet. Therefore, it appears that the wall, which constrains the flow to the region $Z>0$, encourages spillage in the transverse direction. This effect serves to keep the normal growth in the wall jet smaller than that in the free jet and the transverse growth larger. It is noted that, ultimately, in the far field all the wall jets have about equal spread over the plate in the transverse direction.

It was thought that the $e=1.0$ wall jet, which is merely the $e=0.10$ orifice turned onto its narrow end, would behave in a fashion similar to the $e=0.10$ free jet. The fact that the narrow side of the orifice was tangent to the flat plate indicates that the effect of the wall would be least for this case. The velocity profile is shown in

Fig. 42; here, at $X=1$ inch the wall jet results agree very well with those of the free jet. At $X=2$ inches the wall has started to affect the flow (Fig. 43). Note that here the velocity irregularities are present in the normal profile. They are not in the transverse profiles. Indeed, velocity irregularities in turbulent shear flows, as described by Sforza and Trentacoste¹⁵, appear in planes parallel to the plane of the major axis of the flow field. This is a consequence of the vortex superstructure of such flows according to the model offered by Sforza and Trentacoste¹⁵.

I. Flow Visualization

In order to depict the flow pattern for each orifice, the surface of the plate was sprayed with a solution of lampblack and kerosene. By this method it is possible to see the streamline pattern on the surface of the plate and thereby to study the spread of the jet.

Photographs of the surface flow visualization studies for all orifices tested are presented in Figs. 44a-44e. The mixing zones initiated by the spanwise edges of the orifices are clearly visible. Note that near the centerline of the jet the flow pattern in the near field appears well-ordered. The streamwise extent of the wedge-shaped portion of the flow field characterized by this orderliness decreases as the eccentricity of the orifice increases. The fan-shaped areas emanating from the edges of the orifice depict the encroachment of the transverse mixing process upon the "uniform" inner flow. This aspect of end effects in three-dimensional wall jets is well-illustrated by

the surface coating technique.

Another interesting feature of these flow visualization studies is the "spreadability" of the various jet flow fields. These experiments were all conducted at a jet velocity of 208 fps, yet the dispersion of the jets are widely different. It is evident that the $e=1.0$ orifice generates a jet which spreads a larger layer of high momentum (high enough, that is, to move the surface coating) than any of the others tested. This seems logical since the experimental results show that all normal growths are substantially equivalent and that the $e=1.0$ jet had the most rapid maximum velocity decay; hence this jet should spread the most in the transverse direction.

Finally, visualization studies of the wall jet flow fields were conducted in the PIBAL water tunnel facility. No effort was made to match exit Reynolds numbers for the jets. The flow fields were generated by passing dyed water through a scaled-down settling chamber and orifice plate into a clear, still water ambient. The observed flow was generally classified as laminar or turbulent.

Side and top views of turbulent wall jets generated by orifices of $e=0.05$ and 1.0 are shown in Figs. 45a,b and 46a,b, respectively. The spreading effectiveness of the $e=1.0$ jet is amply illustrated.

A three-quarter view of a jet generated by an orifice of $e=0.10$ under laminar and turbulent conditions is presented in Figs. 47a and b, respectively. The enhanced diffusivity of the turbulent flow field is clearly shown.

J. Surface Friction

The experimental determination of skin friction coefficients for three-dimensional wall jets is a tedious task and has been deferred to later studies. Based on the observations reported herein, however, it is possible to indicate what results may transpire when a full study of the skin friction for these cases is completed.

Consider the usual three-dimensional boundary layer equations in the present case of the wall jet:

$$u_X + v_Y + w_Z = 0 \quad (1)$$

$$uu_X + vv_Y + ww_Z = \frac{1}{\rho} [(\tau_{xy})_Y + (\tau_{xz})_Z] \quad (2)$$

where the effect of pressure gradient and the transverse momentum (cross-flow) equations are neglected in this ad hoc analysis. These equations may be combined to yield

$$(u^2)_X + (uv)_Y + (uw)_Z = \frac{1}{\rho} [(\tau_{xy})_Y + (\tau_{xz})_Z] \quad (3)$$

which, when integrated over the area of the half-space bounded by the plate at $Z=0$, yields

$$\int_{-\infty}^{+\infty} \int_0^{\infty} (u^2)_X dy dz = - \int_{-\infty}^{+\infty} (\tau_{xz}/\rho) dy \quad (4)$$

To arrive at this point the following assumptions have been made:

- (i) no slip at the wall;
- (ii) quiescent ambient far from the plate centerline;

(iii) shear symmetry in the XY plane.

Now, by introducing the nondimensional variables

$$\bar{u} = u/u_m, \quad \eta = Y/Y_{1/2}, \quad \text{and} \quad \zeta = Z/Z_{1/2}$$

into Eq. (4), and assuming profile similarity for the mean axial velocity ratio \bar{u} , one obtains

$$M \frac{d\theta}{dX} = \frac{\tau_{w,0} Y_{1/2}}{\rho} \int_{-\infty}^{+\infty} (\tau_w / \tau_{w,0}) d\eta \quad (5)$$

where

$$M = \int_{-\infty}^{+\infty} \int_0^{+\infty} \bar{u}^2 d\eta d\zeta, \quad (6)$$

$$\theta = u_m^2 Y_{1/2} Z_{1/2}, \quad (7)$$

and

$$\tau_{w,0} = \tau_{w,0}(X, 0, 0) .$$

Here the quantity $\tau_w / \tau_{w,0}$ has been introduced in order to set the stage for the keystone assumption of this development, namely, that there exists "shear similarity" in the wall jet flow field, i.e.,

$$\tau_w / \tau_{w,0} = \bar{\tau}_w(\eta) . \quad (8)$$

This assumption appears to be reasonable for the RD region where mean velocity profile similarity is observed, while in the CD region it is

probably inadequate, although it should provide a useful qualitative guide for the present. With these assumptions, the integral momentum flux relation becomes

$$M \frac{d\theta}{dX} = \frac{\tau_{w,o} Y_{\frac{1}{2}}}{\rho} T \quad (9)$$

where

$$T = \int_{-\infty}^{+\infty} \tau_w d\eta \quad (10)$$

Now, in general (see Eq. (7)),

$$\theta \sim X^{-m}, \quad m > 0 \quad (11)$$

with m depending on the region of interest (CD or RD) and the eccentricity of the orifice. Hence one may write

$$d\theta/dX = -m\theta/X \quad (12)$$

Using Eqs. (7) and (12) in Eq. (9), one obtains for the centerline wall shear

$$\tau_{w,o} = m(M/T) \rho u_m^2 \frac{Z_{\frac{1}{2}}}{X} \quad (13)$$

Then the skin friction coefficient

$$C_{f,o} = \tau_{w,o} / \frac{1}{2} \rho u_m^2 = 2m(M/T) \frac{Z_{\frac{1}{2}}}{X} \quad (14)$$

Of interest here is the fact that $Y_{\frac{1}{2}}$ does not appear in the skin

friction coefficient for the three-dimensional wall jet; the lateral spread of the jet, to this approximation, alters the magnitude of $C_{f,0}$ but not its streamwise variation. It was previously shown that

$$Z_{1/2} \sim X^b \quad (15)$$

This result, when coupled with the Reynolds number based on the normal half-width

$$(Re)_{1/2} \sim Re_m = \frac{u_m Z_m}{\nu} \sim X^c, \quad (16)$$

may be utilized to determine the variation of centerline skin friction coefficient with streamwise distance X or maximum Reynolds number Re_m as shown below:

$$C_{f,0} = K \frac{Z_{1/2}}{X} \sim X^r \sim Re_m^w. \quad (17)$$

Eq. (17) is the skin friction coefficient at the wall and along the centerline of the flow for a wall jet having shear similarity. Tables I and II compare $C_{f,0}$, the $Z_{1/2}$ half-width growth, and the maximum velocity decay for the 2-D, radial, and 3-D wall jets. The streamwise dependence of the skin friction coefficient is calculated from Eq. (17), using the data of past investigators and compared with their result.

Bradshaw and Gee⁴ found that the so-called two-dimensional value, $C_{f,2-D} \sim X^{-.069}$ and, using their data, Eq. (17) yields $C_{f,0} \sim X^{-.09}$. For a radial wall jet Poreh, et al.⁵ determined the skin friction coefficient decay to be proportional to $X^{-.10}$, which is in exact agreement with

the result obtained by using their data and assuming shear similarity, i.e., solving for $C_{f,0}$ by Eq. (17). This supports the assumption that perhaps such similarity does indeed exist for a wall jet type flow, especially in the RD region. A more precise experimental validation of this concept of shear similarity appears to be a worthwhile endeavor.

IV. CONCLUDING REMARKS

An experimental study of the bulk properties of turbulent, three-dimensional, incompressible wall jets issuing into a quiescent air ambient has been presented. The results obtained indicate some characteristics of such flow fields and their relationship to flows dependent upon only two space coordinates. Comparisons with the free jet counterparts were also discussed.

The more interesting results may be listed as follows:

- (1) These flow fields are characterized by three regions defined by the maximum velocity decay rate.
- (2) The maximum velocity decay rate becomes oblivious of orifice geometry as the flow proceeds downstream; it eventually takes on the value found for radial wall jets.
- (3) The half-width growth normal to the plate is independent of orifice geometry while that transverse to the plate is influenced by the orifice shape until stations very far downstream from the exit are reached.
- (4) Velocity nonuniformities in the transverse direction were observed in the near field of jets emanating from slender rectangular orifices. This feature suggests that the characterization of flow fields generated by slender slots as quasi-two-dimensional may be of questionable validity.

The centerline shear stress distribution along the wall was obtained from an integral analysis of the boundary layer equations by

assuming shear similarity in the flow. The results obtained agree reasonably well with those found experimentally. A further study to determine more accurately the validity of the shear similarity assumption was suggested.

V. REFERENCES

1. Viets, H. and Sforza, P.M.: An Experimental Investigation of a Turbulent, Incompressible, Three-Dimensional Wall Jet. Polytechnic Institute of Brooklyn, PIBAL Report No. 968, AFOSR 66-0888, April 1966.
2. Sigalla, A.: Measurements of Skin Friction in a Plane Turbulent Wall Jet. J. of Roy. Aero. Soc., 62, p. 873, 1958.
3. Bakke, P.: An Experimental Investigation of a Wall Jet. J. Fluid Mech., 2, p. 467, 1957.
4. Bradshaw, P. and Gee, M.T.: Turbulent Wall Jets With and Without an External Stream. Aero. Res. Council R & M No. 3252, 1962.
5. Poreh, M., Tsuei, Y.G., and Cermak, J.E.: Investigation of a Turbulent Radial Wall Jet. J. Appl. Mech., Trans. ASME, pp. 457-463, June 1967.
6. Sawyer, R.E.: The Flow Due to a Two-Dimensional Jet Issuing Parallel to a Flat Plate. J. Fluid Mech., 9, pt. 4, 1961.
7. Schwarz, W.H. and Cosart, W.P.: The Two-Dimensional Turbulent Wall Jet. J. Fluid Mech., 10, pt. 4, June 1961.
8. Kruka, V. and Eskinazi, S.: The Wall Jet in a Moving Stream. J. Fluid Mech., 20, pt. 4, pp.555-579, 1964.
9. Gartshore, I.S.: Jets and Wall Jets in Uniform Streaming Flow. McGill University, Mechanical Engineering Laboratories, Report 64-4, May 1964.

10. Gartshore, I.S. and Hawaleshka, O.: The Design of a Two-Dimensional Blowing Slot and Its Application to a Turbulent Wall Jet in Still Air. McGill University, Mechanical Engineering Laboratories, Report 64-5, June 1964.
11. Gartshore, I.S.: The Streamwise Development of Certain Two-Dimensional Turbulent Shear Flows. McGill University, Mechanical Engineering Laboratories, Report 65-3, April 1965.
12. Pajaratnam, N. and Subramanya, K.: An Annotated Bibliography on Wall Jets. University of Alberta, Dept. of Civil Engineering, July 1967.
13. Sforza, P.M., Steiger, M.H., and Trentacoste, N.: Studies on Three-Dimensional Viscous Jets. AIAA J., 4, 5, pp. 800-806, May 1966.
14. Trentacoste, N. and Sforza, P.M.: An Experimental Investigation of Three-Dimensional Free Mixing in Incompressible, Turbulent Free Jets. Polytechnic Institute of Brooklyn, PIBAL Report No. 871, AFOSR 66-0651, March 1966.
15. Sforza, P.M. and Trentacoste, N.: Mean Flow Nonuniformities in Three-Dimensional Turbulent Shear Flows. Polytechnic Institute of Brooklyn, PIBAL Report No. 975 (to be issued).
16. Glauert, M.B.: The Wall Jet. J. Fluid Mech., 1, p. 625, 1956.
17. Chao, J.L. and Sandborn, V.A.: Evaluation of the Momentum Equation for a Turbulent Wall Jet. J. Fluid Mech., 26, pt. 4, pp. 819-828, 1956.

18. Nishimura, Y.: Application of a Jet Pump and Coanda Surface to Ventilation of a Highway Tunnel. University of Toronto, Institute for Aerospace Studies, UTIAS TN-82, February 1965.
19. Tuve, G.L., Priester, G.B., and Wright, D.K.: Entrainment and Jet-Pump Action of Air Streams. J. Heating and Ventilation, 48, No. 1204, pp. 241-266, 1942.
20. Manganiello, E.J. and Bogatsky, D.: An Experimental Investigation of Rectangular Exhaust Gas Ejectors Applicable for Engine Cooling. NASA WRE-224, May 1944.

TABLE I

Type of Flow Field	Investigators	Streamwise variation of half-width growth Normal to plate ($Z_{1/2}$)	Spanwise ($Y_{1/2}$)	Axial decay of maximum mean velocity (u_0)
"Two-Dimensional" wall jet	Sigalla ²	$X^{1.0}$	---	$X^{-0.50}$
	Bradshaw & Gee ⁴	$X^{0.91}$	---	$X^{-0.53}$
	Schwarz & Cosart ⁷	$X^{1.0}$	---	$X^{-0.55}$
Radial wall jet	Bakke ³	$X^{0.94}$	---	$X^{-1.12}$
	Poreh, et al. ⁵	$X^{0.9}$	---	$X^{-1.1}$
Three-Dimensional wall jet	Present results	$X^{0.78 \pm 0.07}$ (for all conventional orifices tested, in both CD & RD regions)	<u>CD region</u>	
			$e=0.025 : X^{-0.41}$	
			$e=0.05 : X^{-0.43}$	
			<u>RD region</u>	
			$X^{-1.1}$	
			(all conventional orifices tested)	

TABLE II

Flow Field	Investigators	Streamwise variation of skin friction coefficient: measured values	Streamwise variation of skin friction coefficient; calculated from Eq. (17)	Variation of skin friction coefficient with Reynolds number
Two-dimensional wall jet	Sigalla ²	$X^{-0.125}$	constant	constant
	Bradshaw & Gee ⁴	$X^{-0.069}$	$X^{-0.09}$	$Re_m^{-0.24}$
	Schwarz & Cosart ⁷	$X^{-0.111}$	constant	constant
Radial wall jet	Bakke ³	---	$X^{-0.06}$	$Re_m^{0.33}$
	Poreh, et al. ⁵	$X^{-0.10}$	$X^{-0.10}$	$Re_m^{0.50}$
Three-dimensional wall jet	Present results	---	$X^{-0.22 \pm 0.07}$	$\frac{CD}{Re_m}$ Region $e=0.025:Re_m^{-0.59}$
			(all conventional orifices tested in both CD & RD regions)	$e=0.05:Re_m^{-0.63}$
				$e=0.10:Re_m^{-0.36}$
			$\frac{RD}{Re_m}$ Region 0.69 ± 0.09	

(all conventional orifices tested)

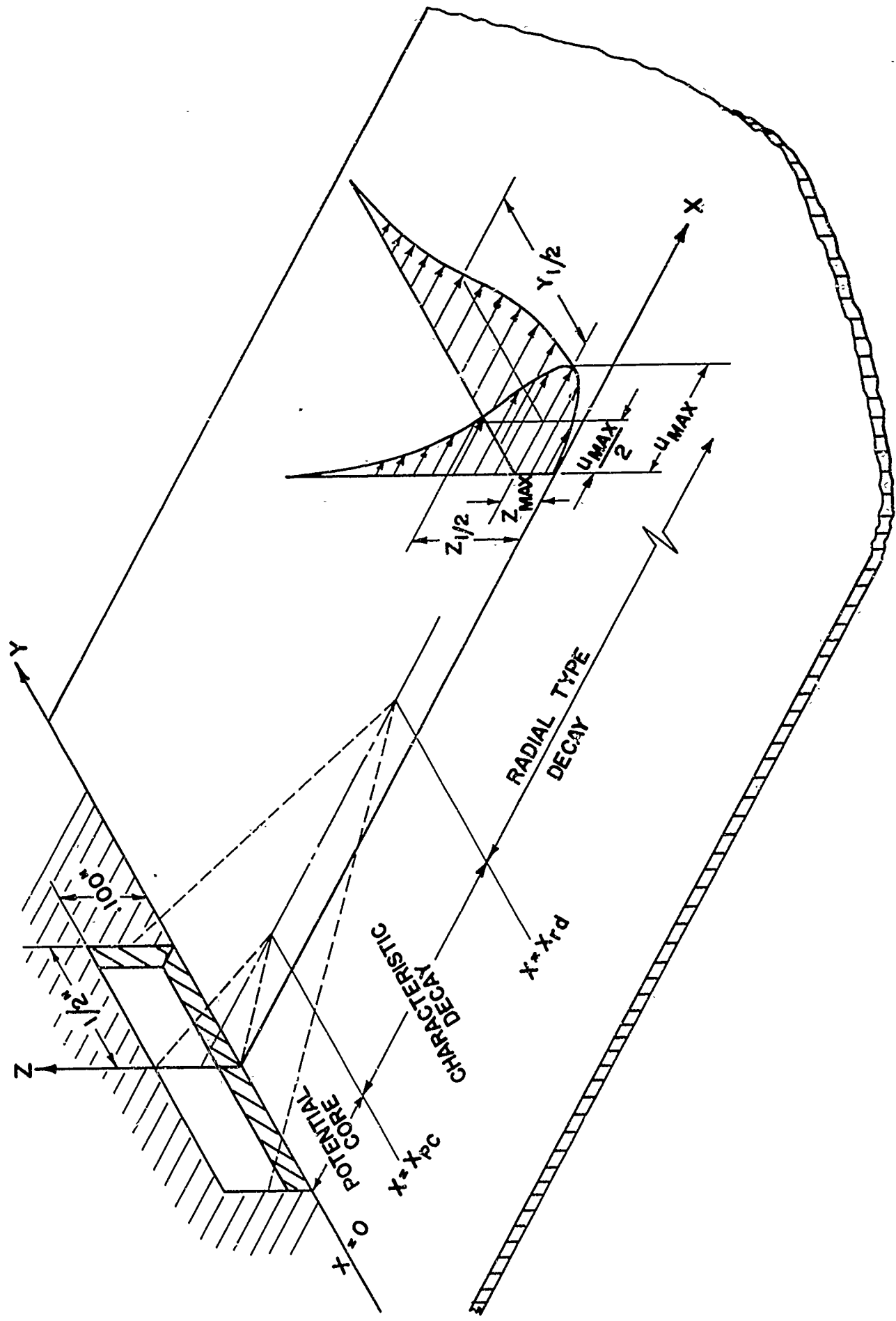


FIG. 1 SCHEMATIC REPRESENTATION OF FLOW FIELD OF 3 DIMENSIONAL WALL JET

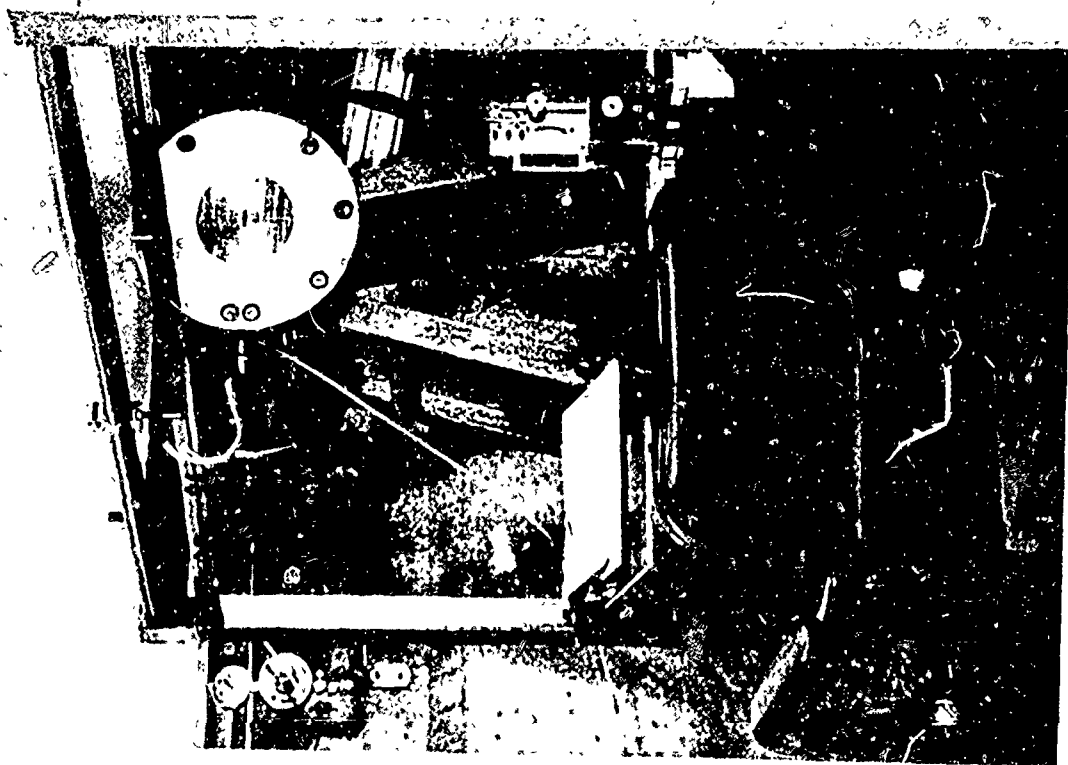


FIG. 2 WALL JET TEST FACILITY

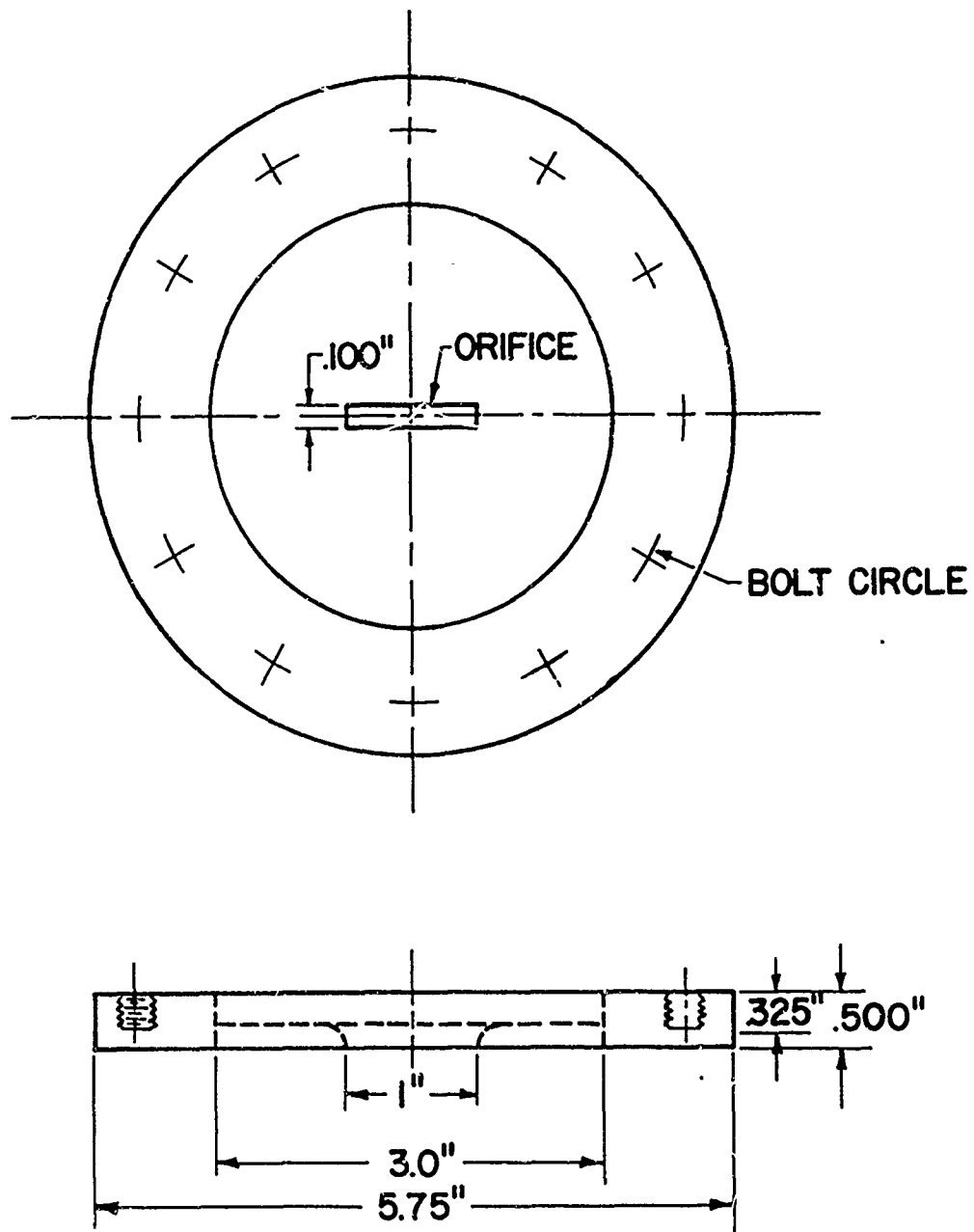


FIG. 3 END CAP SCHEMATIC

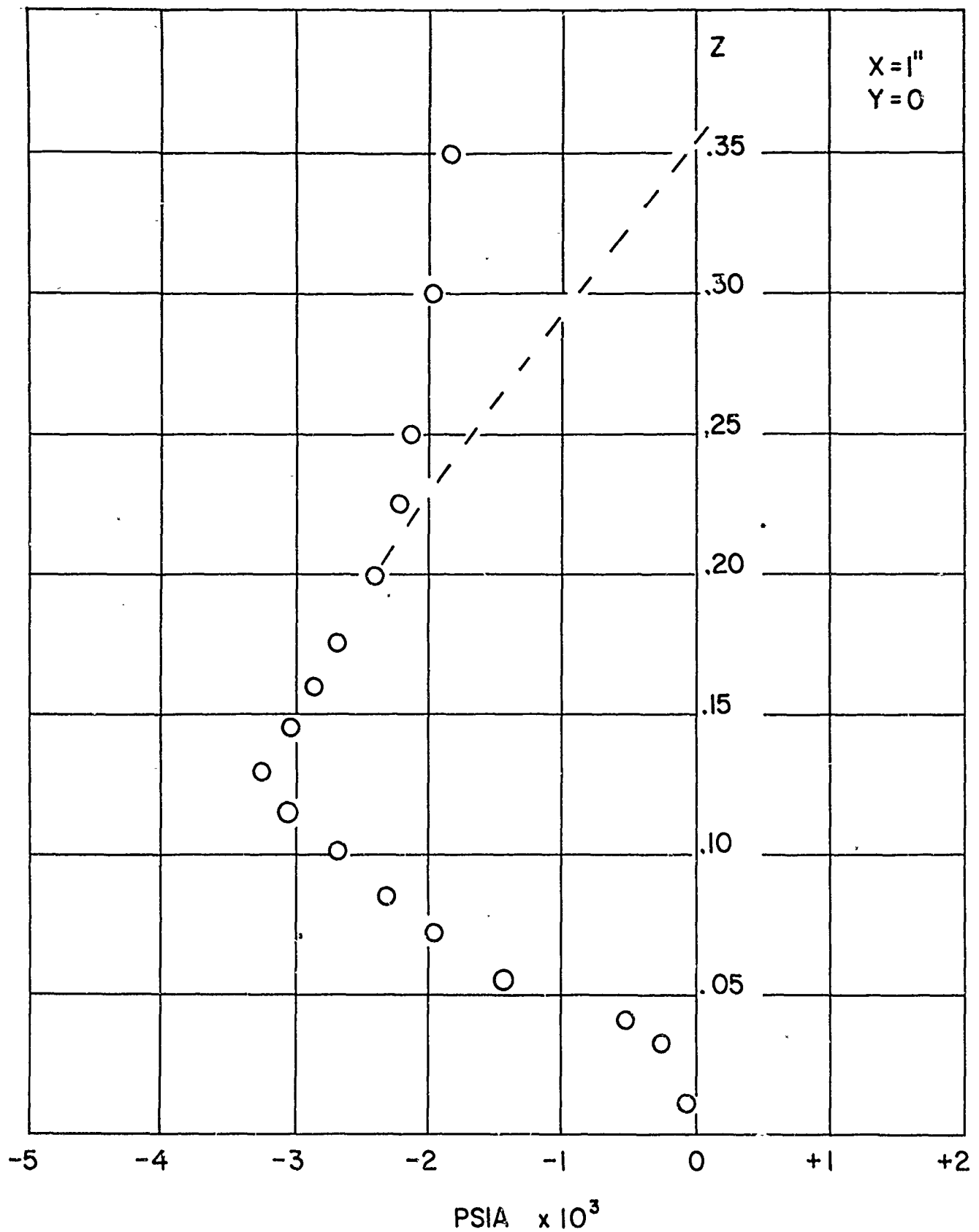
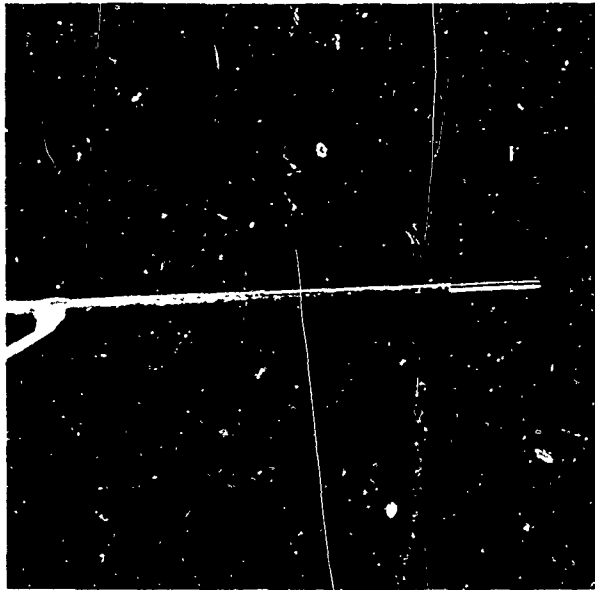


FIG. 4 STATIC PRESSURE DISTRIBUTION ($e = .10$)

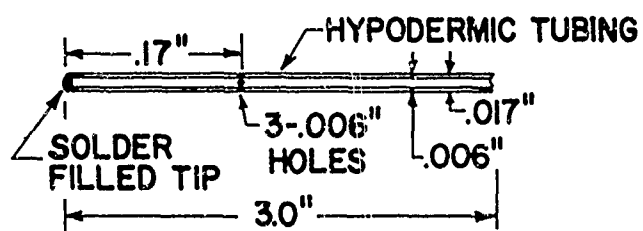
(THE PRESSURE DOES NOT RETURN TO EXACTLY AMBIENT PRESSURE DUE TO WETTING OF THE MANOMETER TUBE SURFACE)



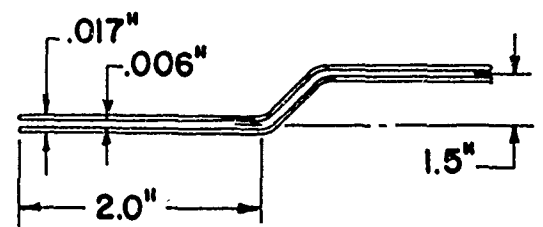
CLOSEUP, PROBE 2



OVERALL VIEW, PROBE 1



PROBE - 2



PROBE - 1

FIG. 5 DETAILS OF PROBE DESIGN

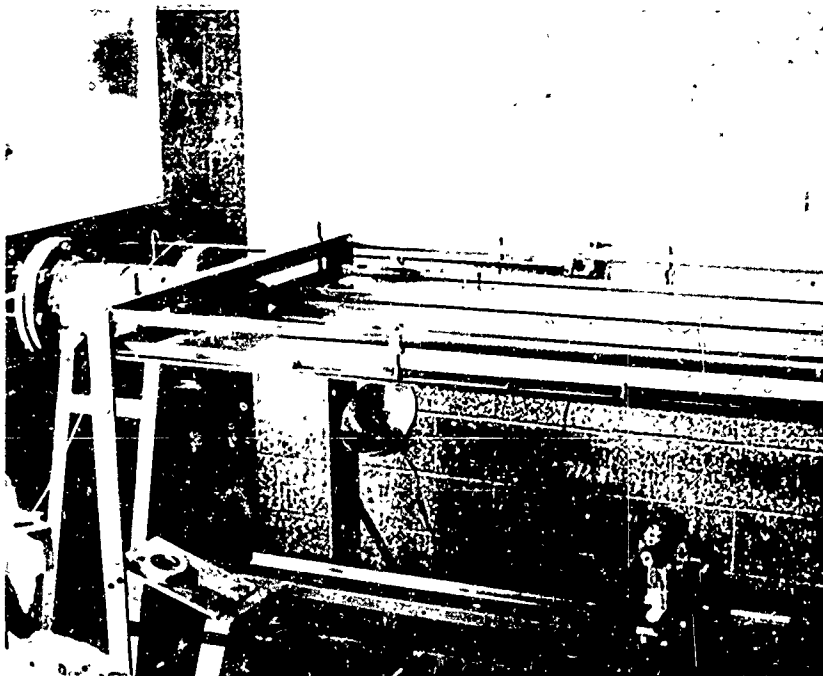


FIG. 6 VIEW OF FRAMEWORK FOR ADJUSTMENT OF WALL FLATNESS IN WALL JET FACILITY

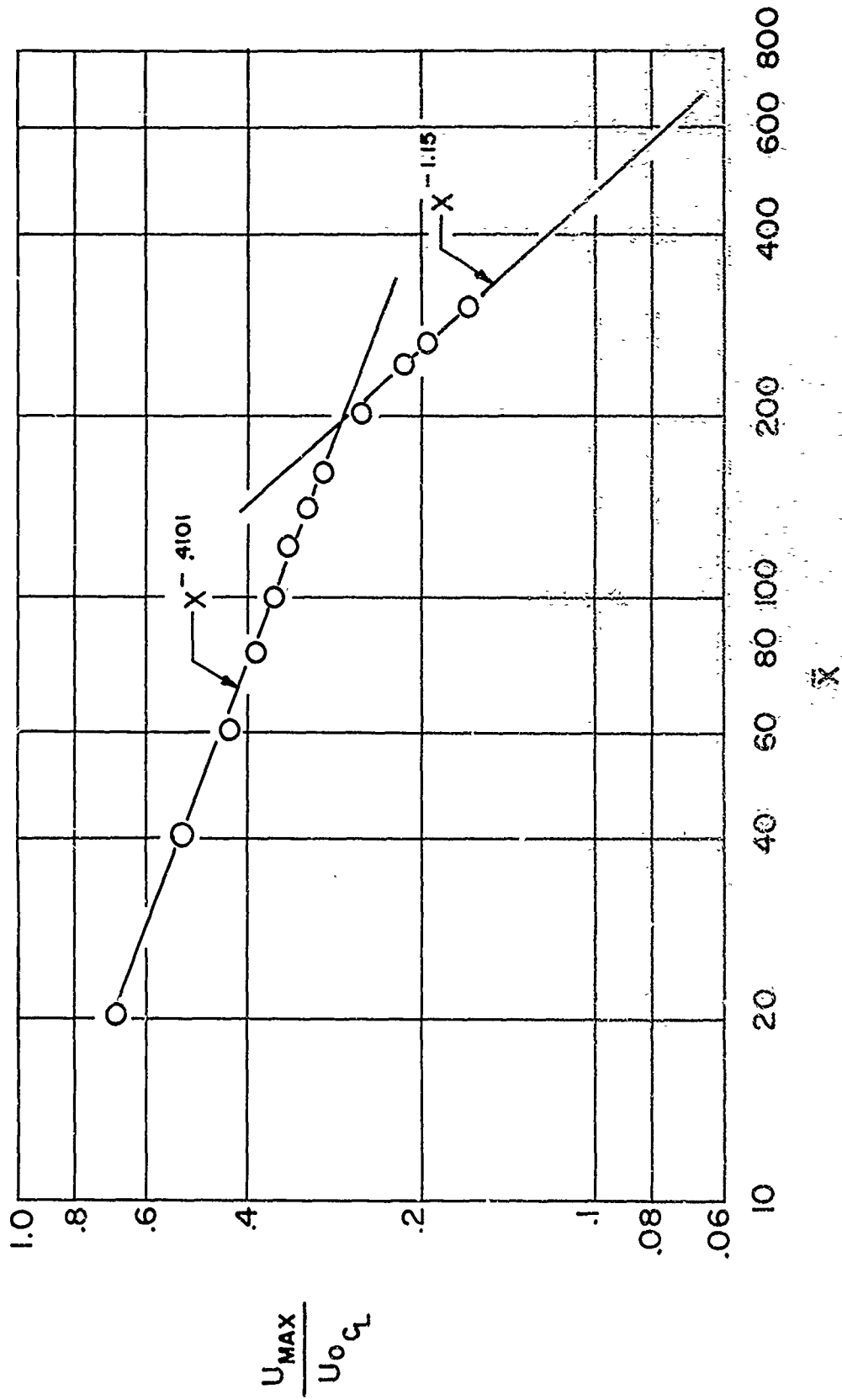


FIG. 7 MAXIMUM VELOCITY DECAY FOR $e = .025$

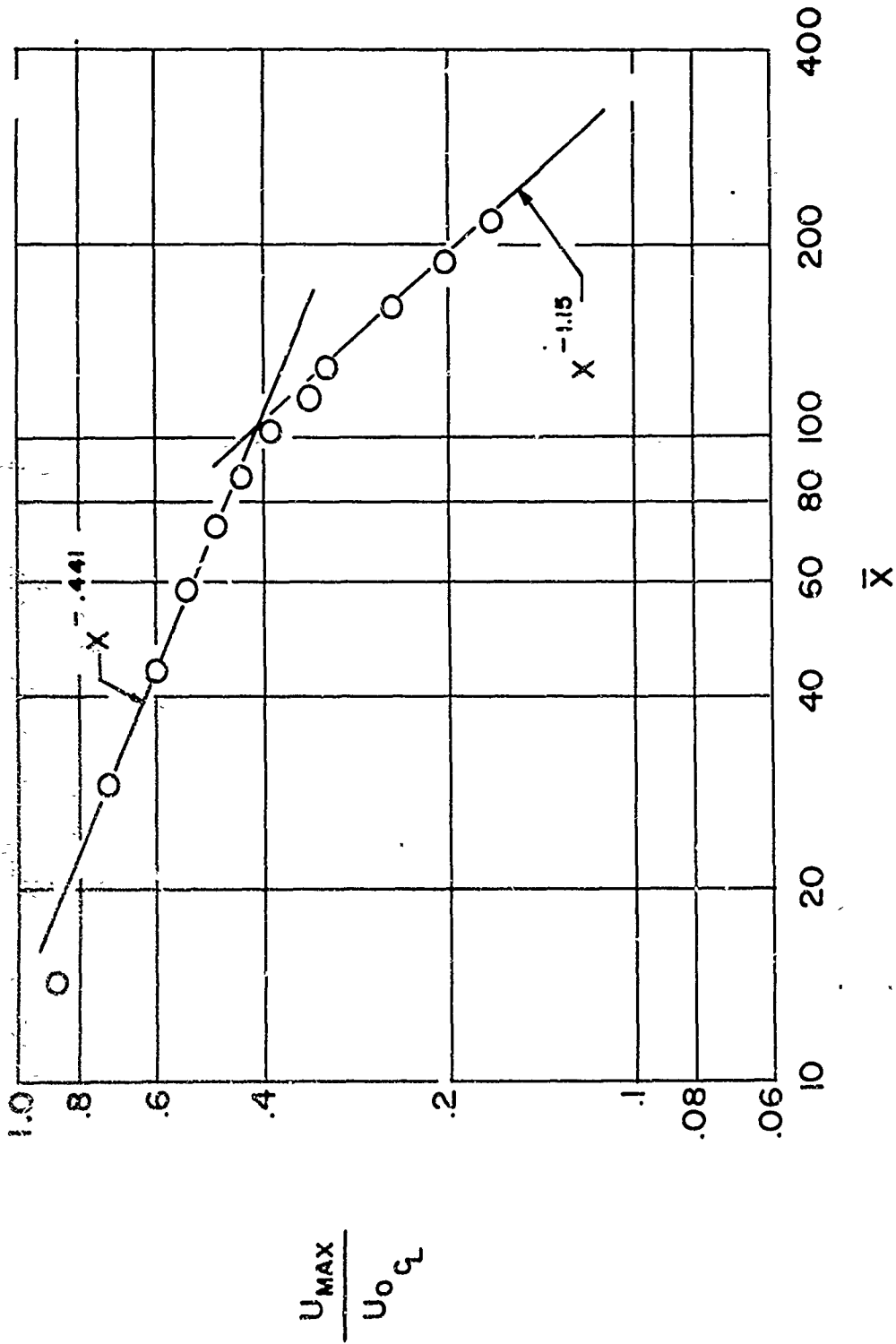


FIG. 8 MAXIMUM VELOCITY DECAY FOR $e=0.05$

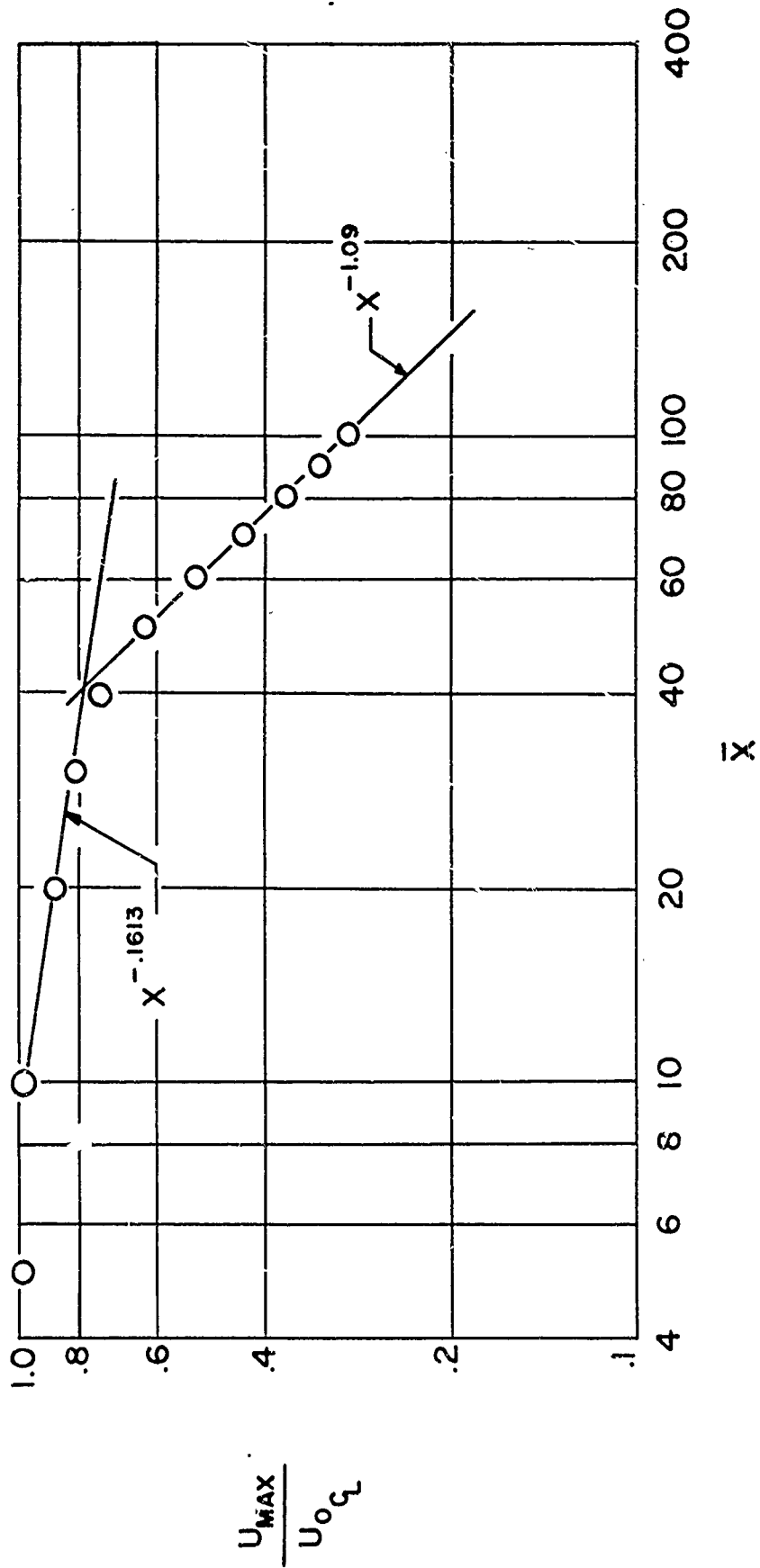


FIG. 9 MAXIMUM VELOCITY DECAY FOR $e=1.0$

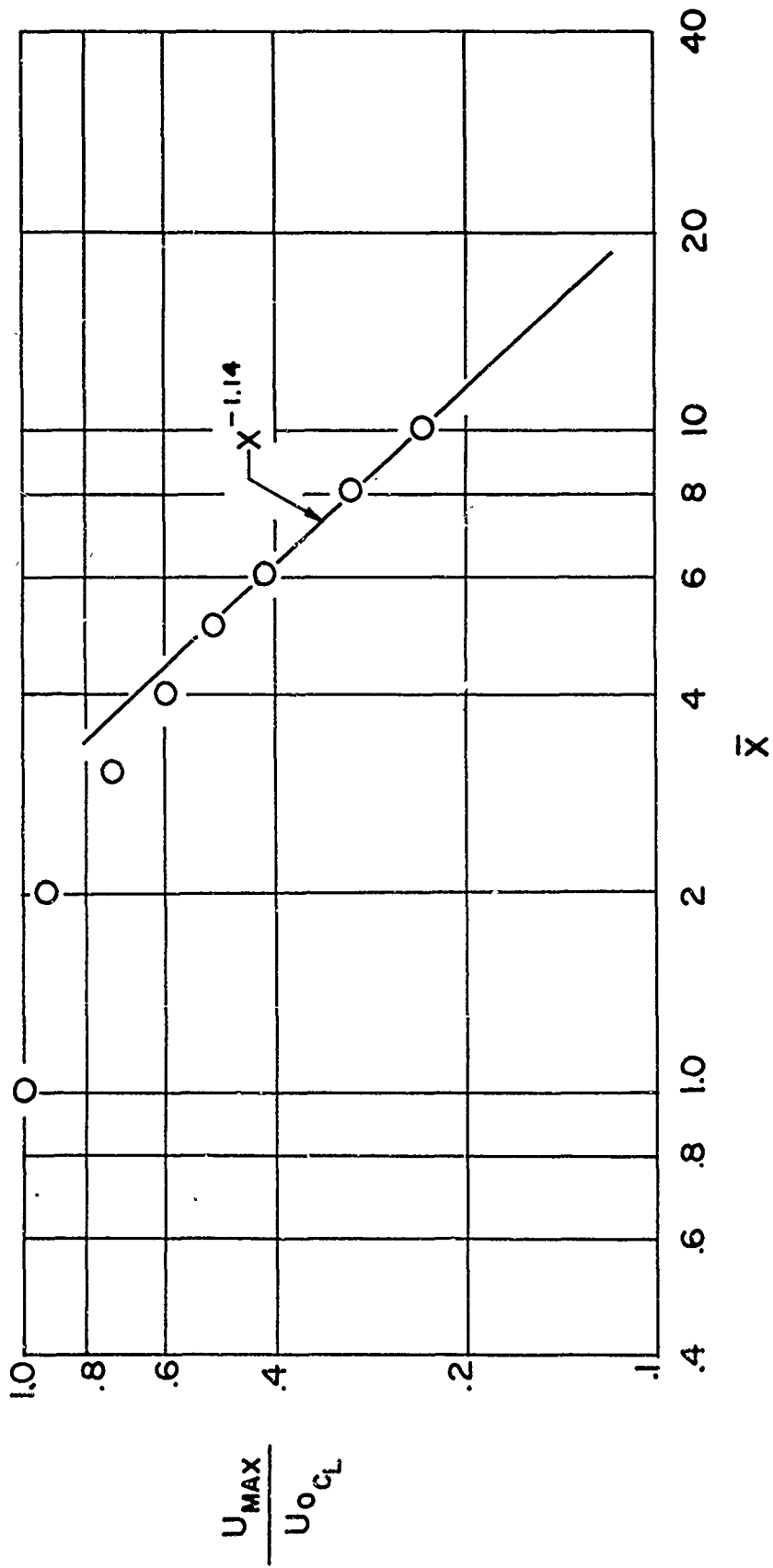


FIG. 10. MAXIMUM VELOCITY DECAY FOR $e = 1.0$

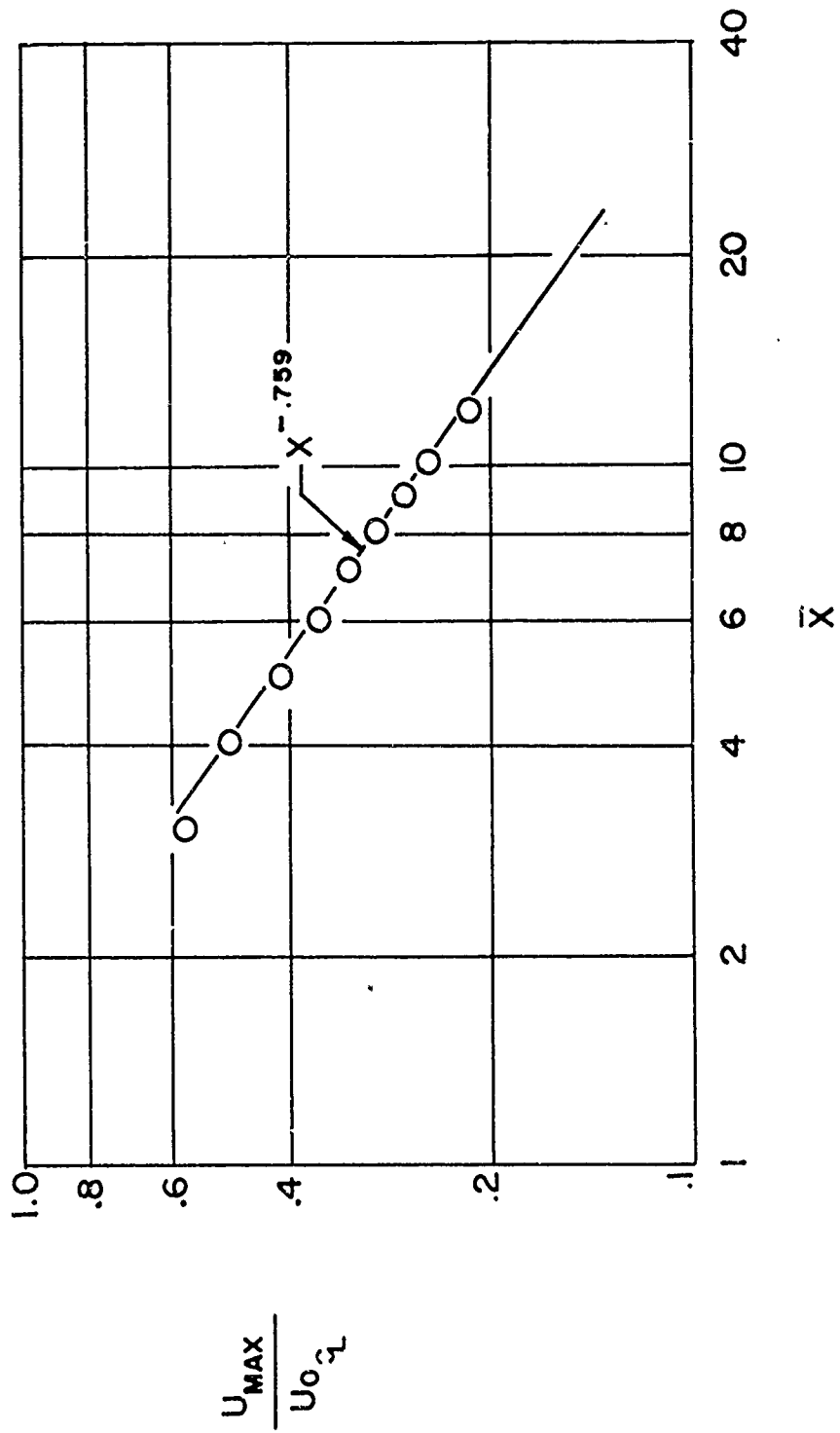


FIG. 11 MAXIMUM VELOCITY DECAY FOR $e = 10$

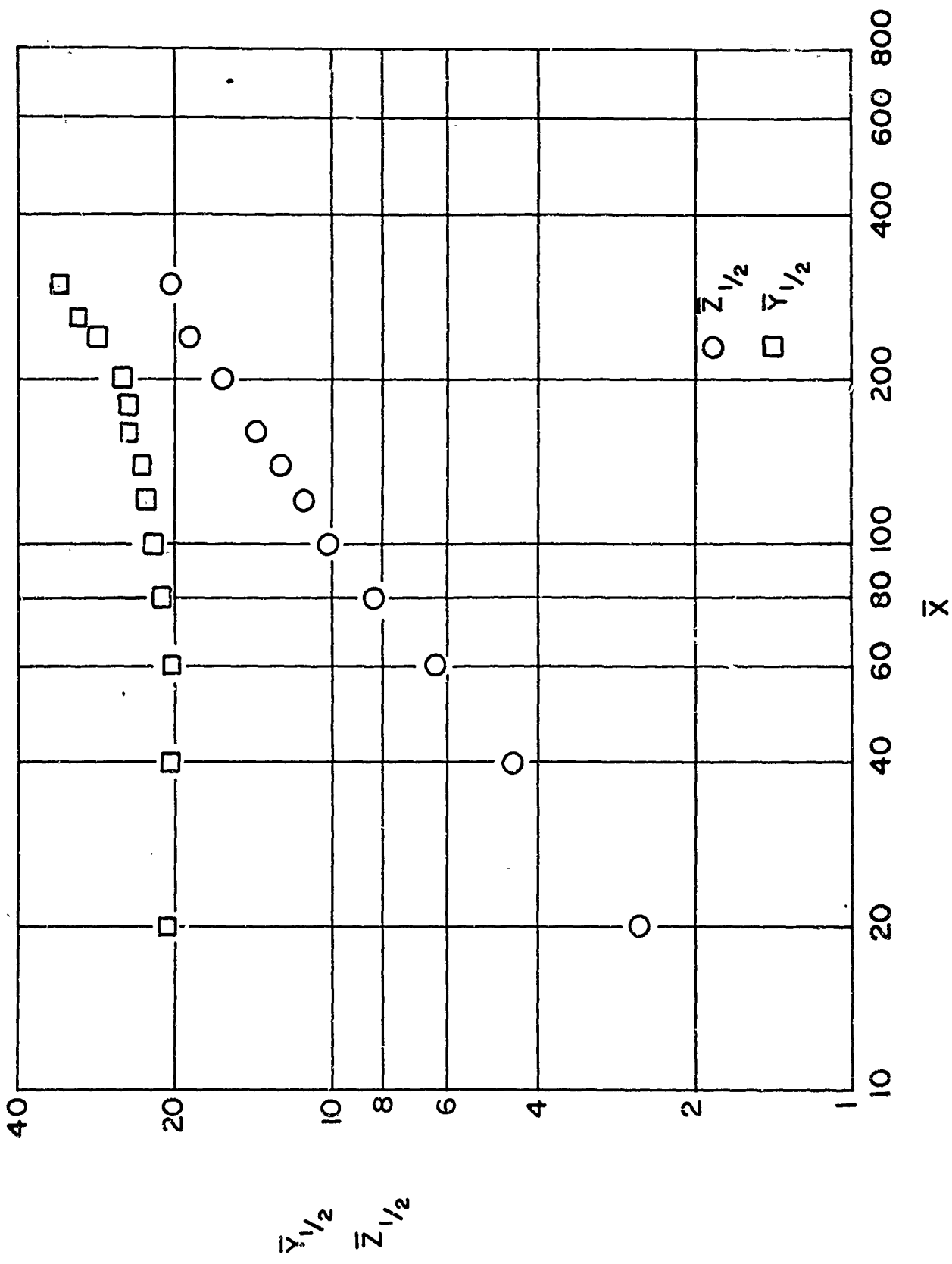


FIG. 12 HALF WIDTH GROWTH FOR $e = .025$

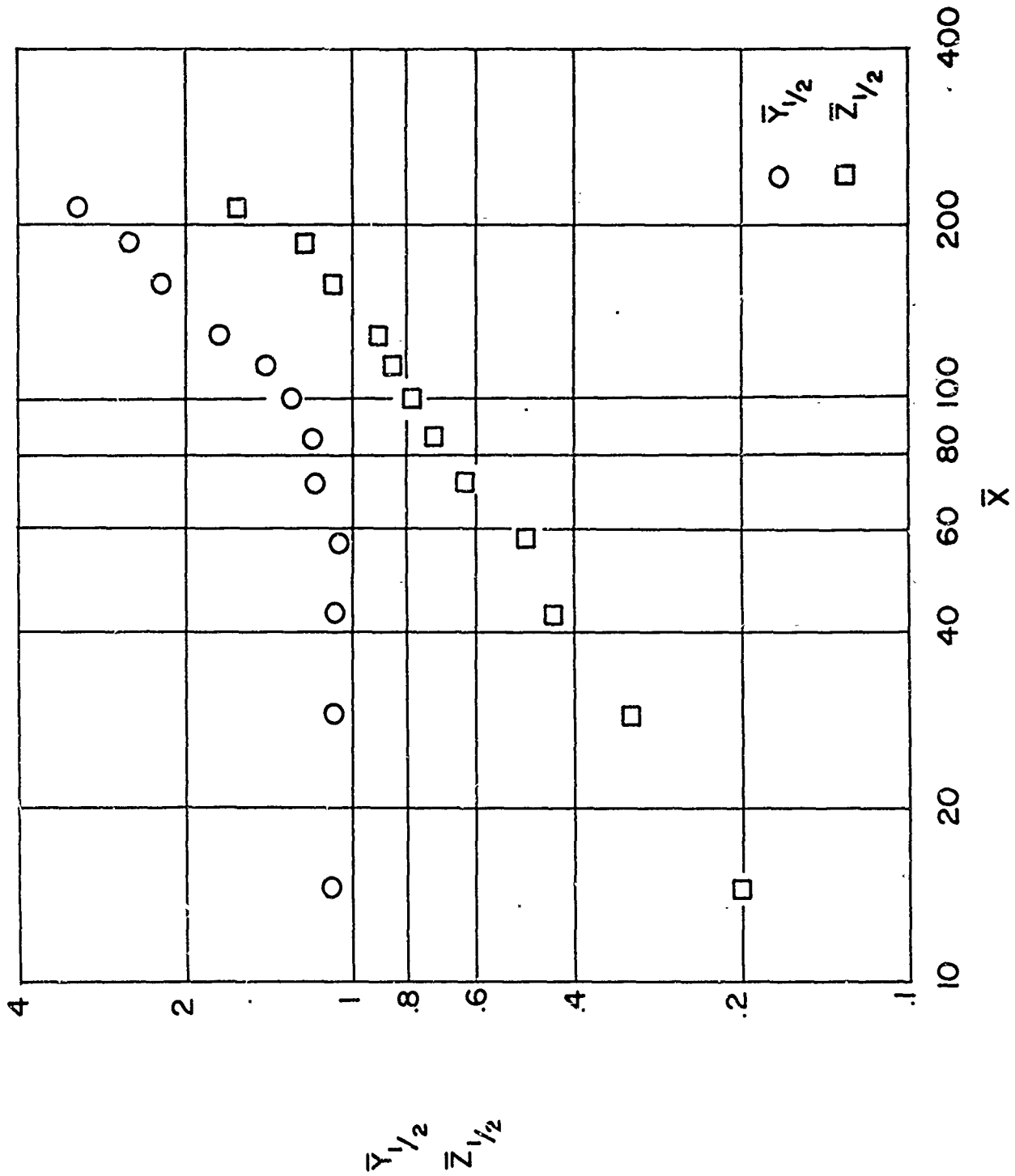


FIG. 13 HALF WIDTH GROWTH FOR $e = .05$

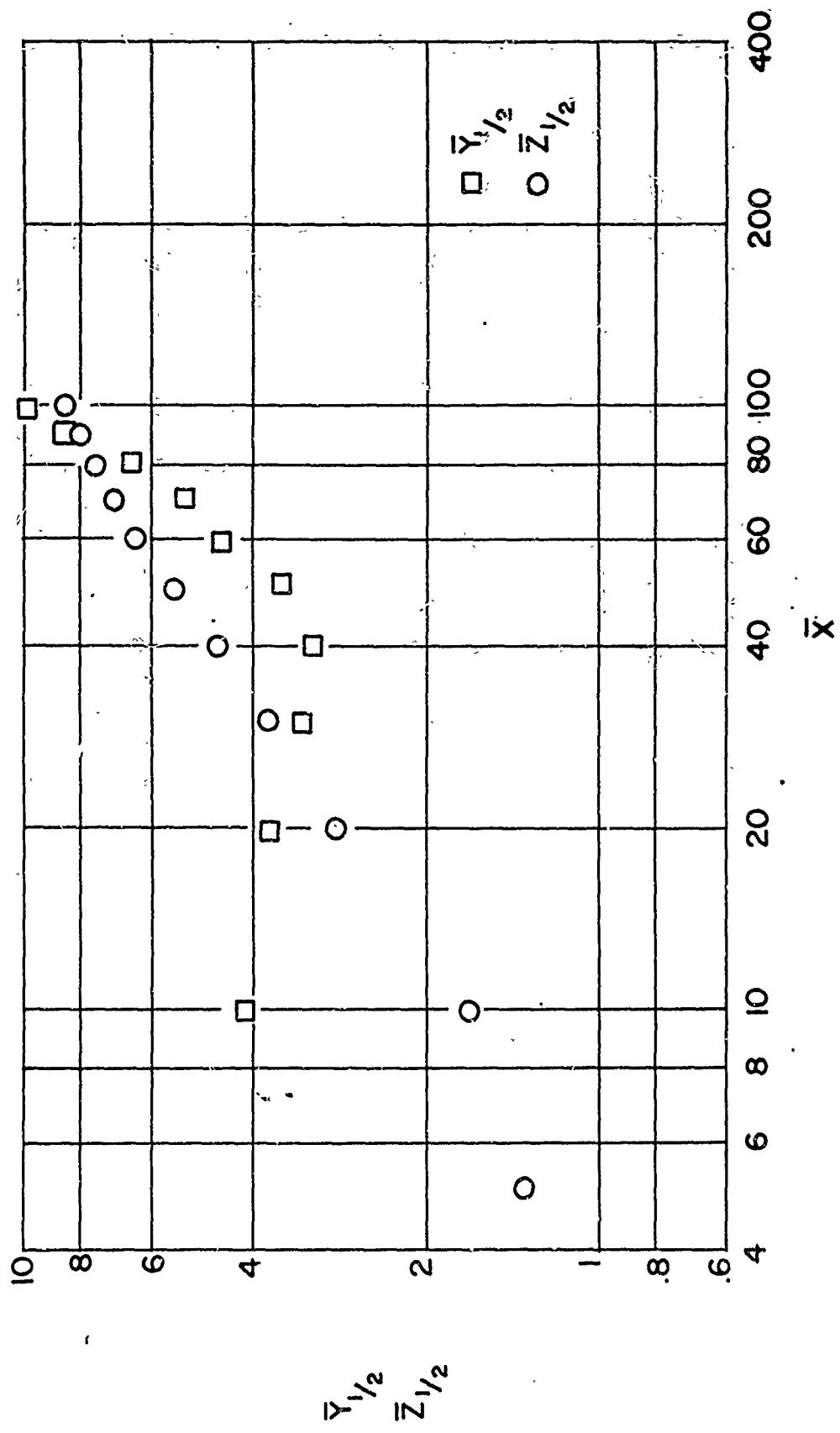


FIG. 14 HALF WIDTH GROWTH FOR $e = .10$

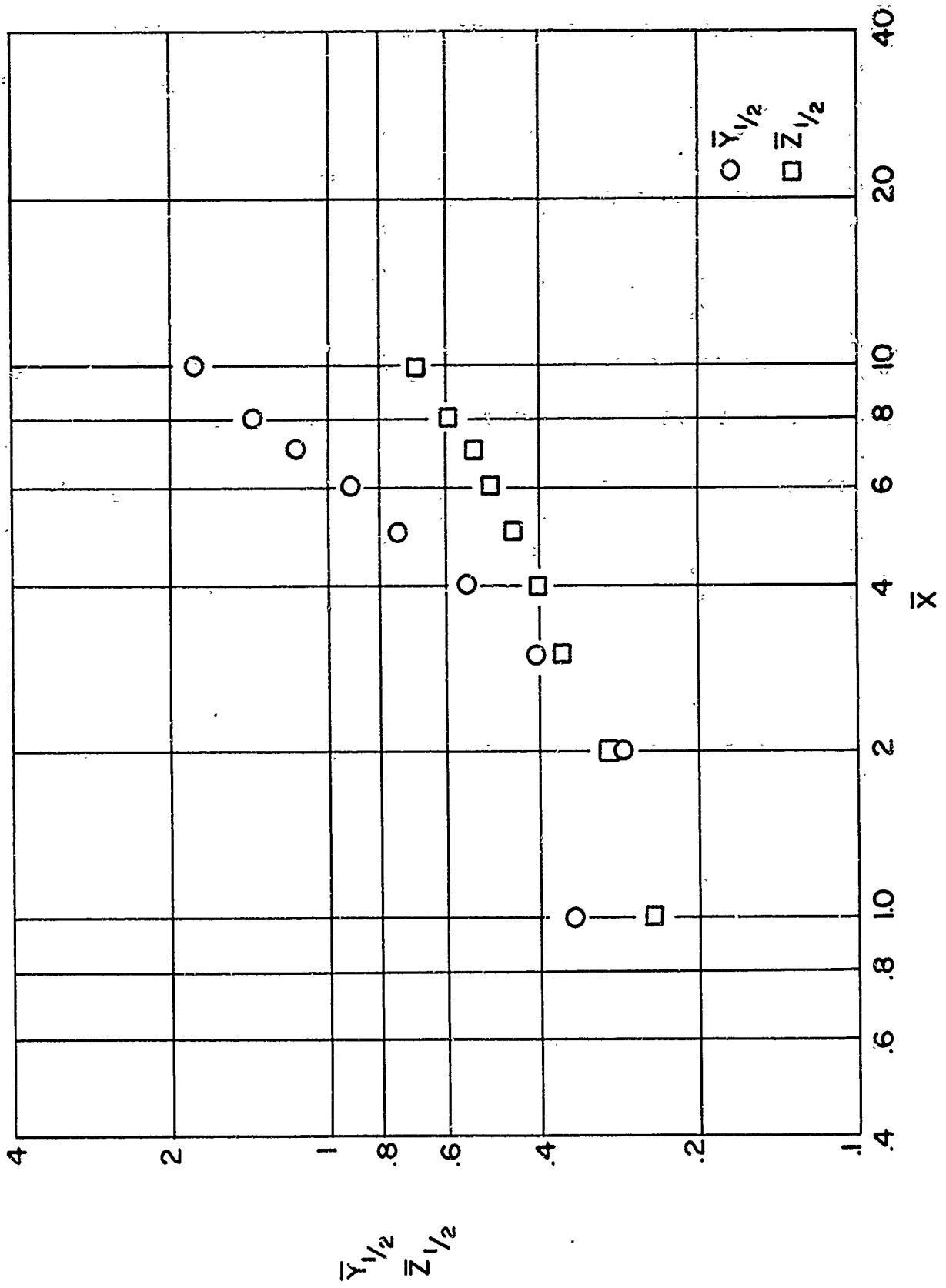


FIG. 15 HALF WIDTH GROWTH FOR $e=1.0$

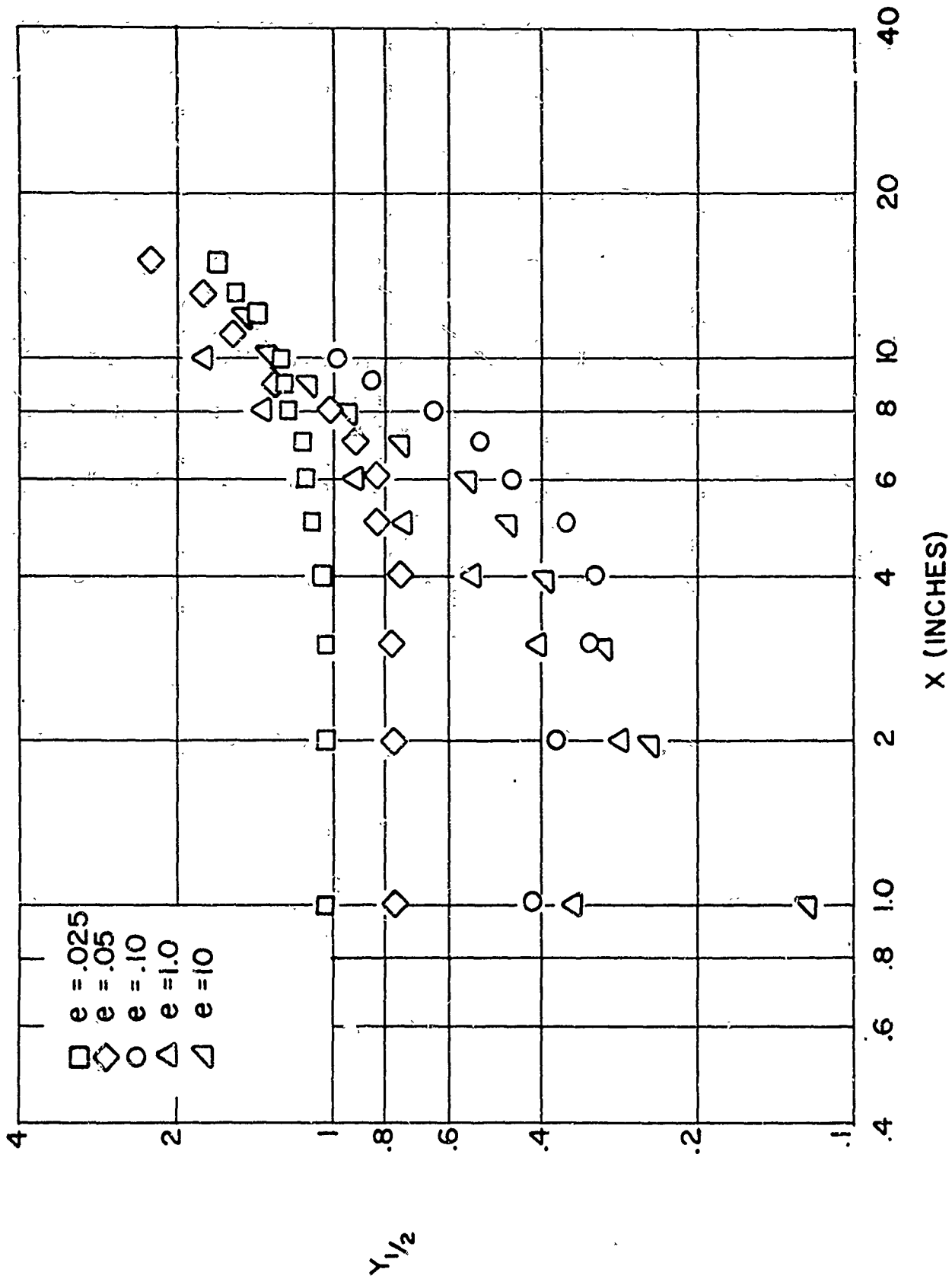


FIG. 16 COMPOSITE OF $Y_{1/2}$ FOR ALL WALL JETS TESTED

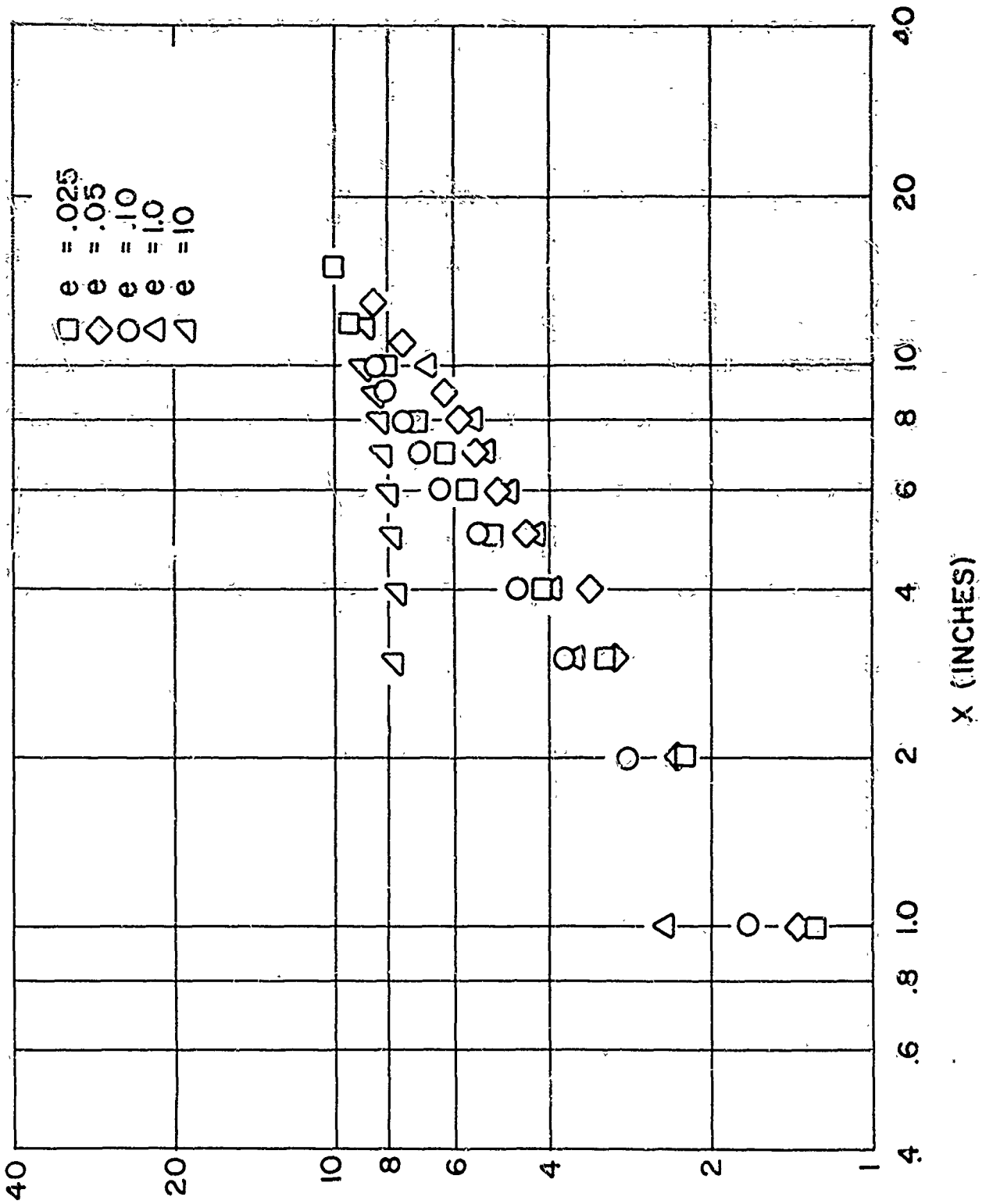


FIG. 17 COMPOSITE OF $Z_{1/2}$ FOR ALL WALL JETS TESTED

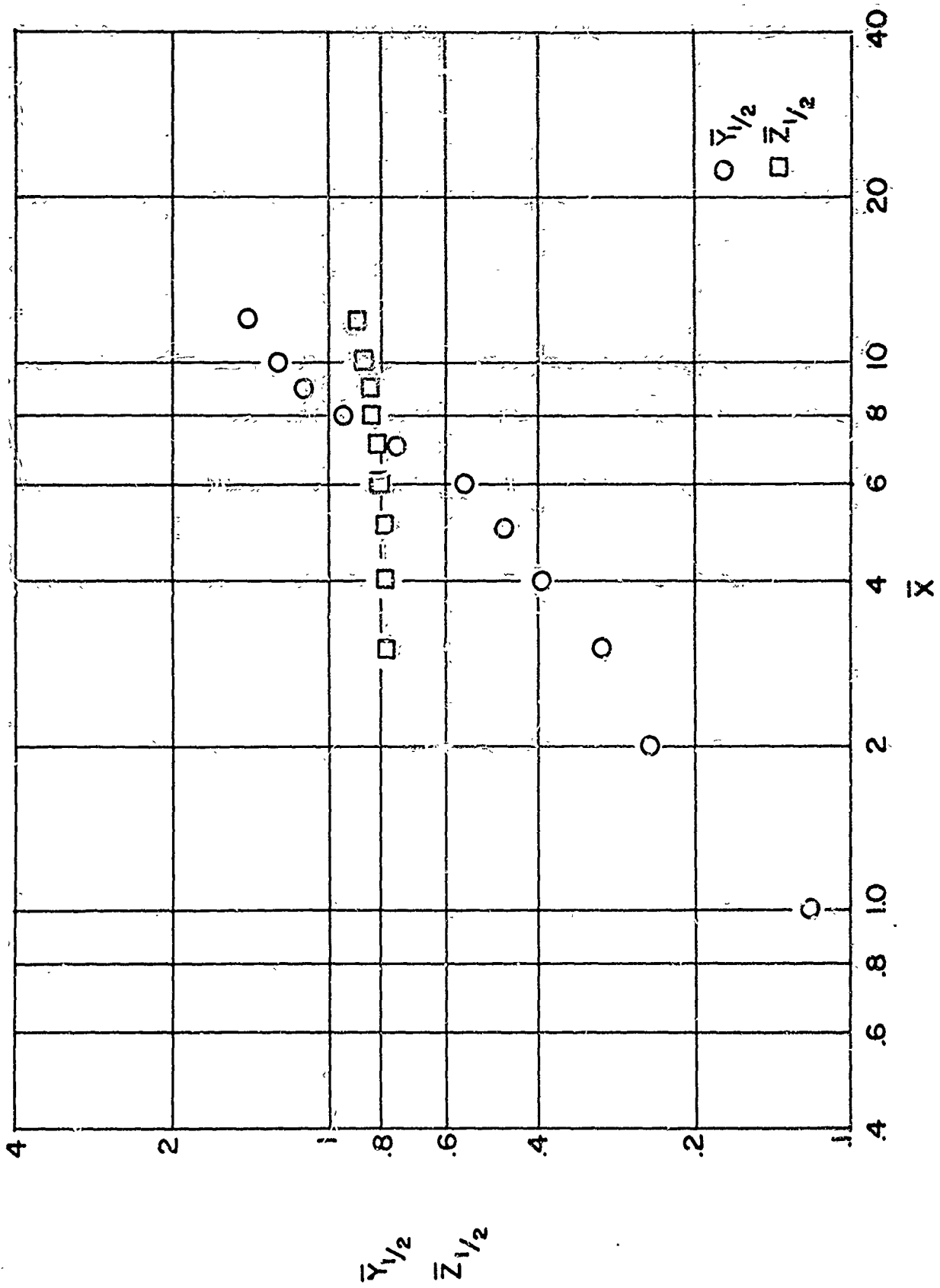


FIG. 18 HALF WIDTH GROWTH FOR $e = 10$

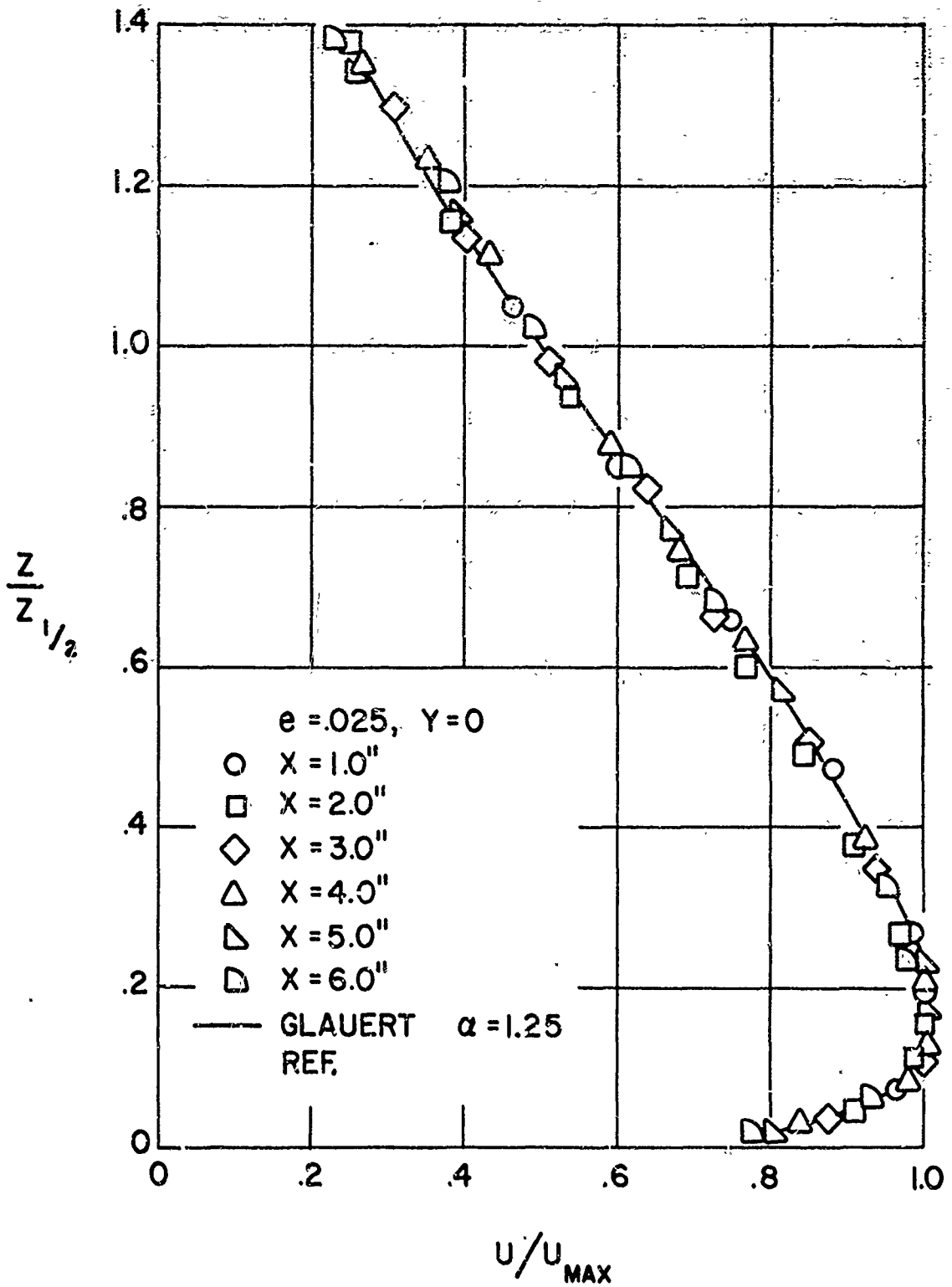


FIG. 19 AXIAL VELOCITY PROFILES IN CHARACTERISTIC DECAY REGION

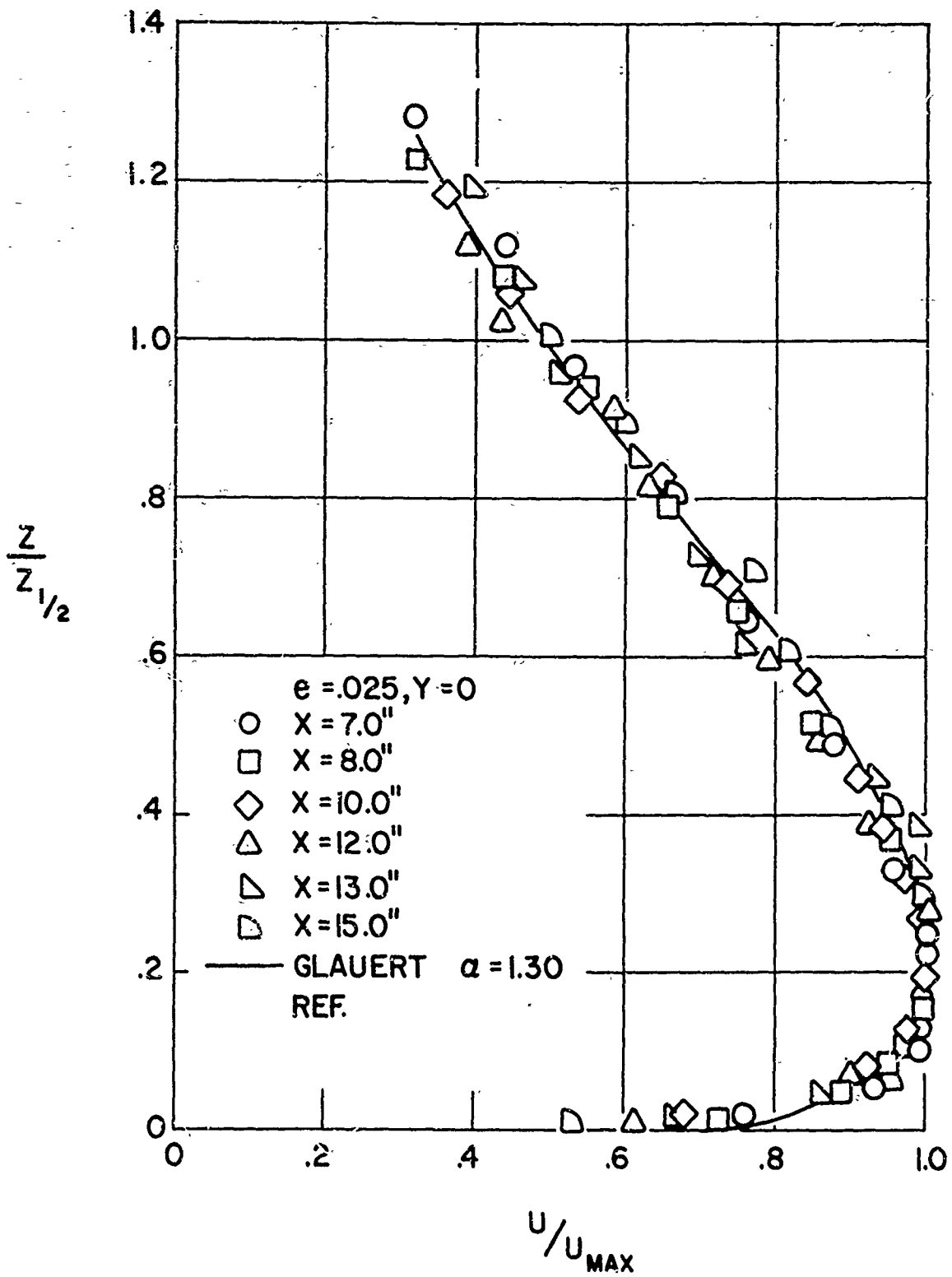


FIG.20 AXIAL VELOCITY PROFILES IN RADIAL TYPE DECAY REGION

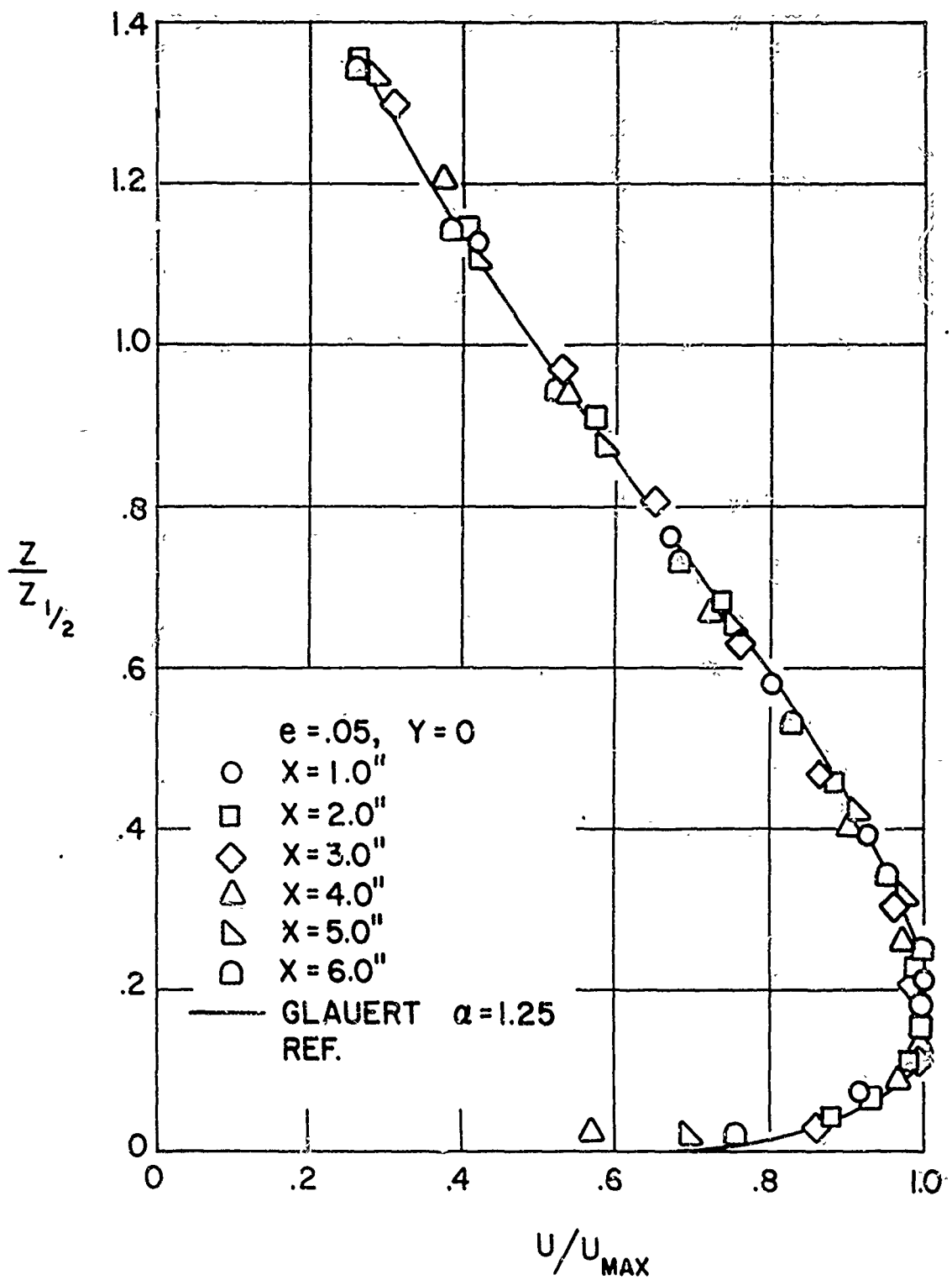


FIG. 21 AXIAL VELOCITY PROFILES IN CHARACTERISTIC DECAY REGION

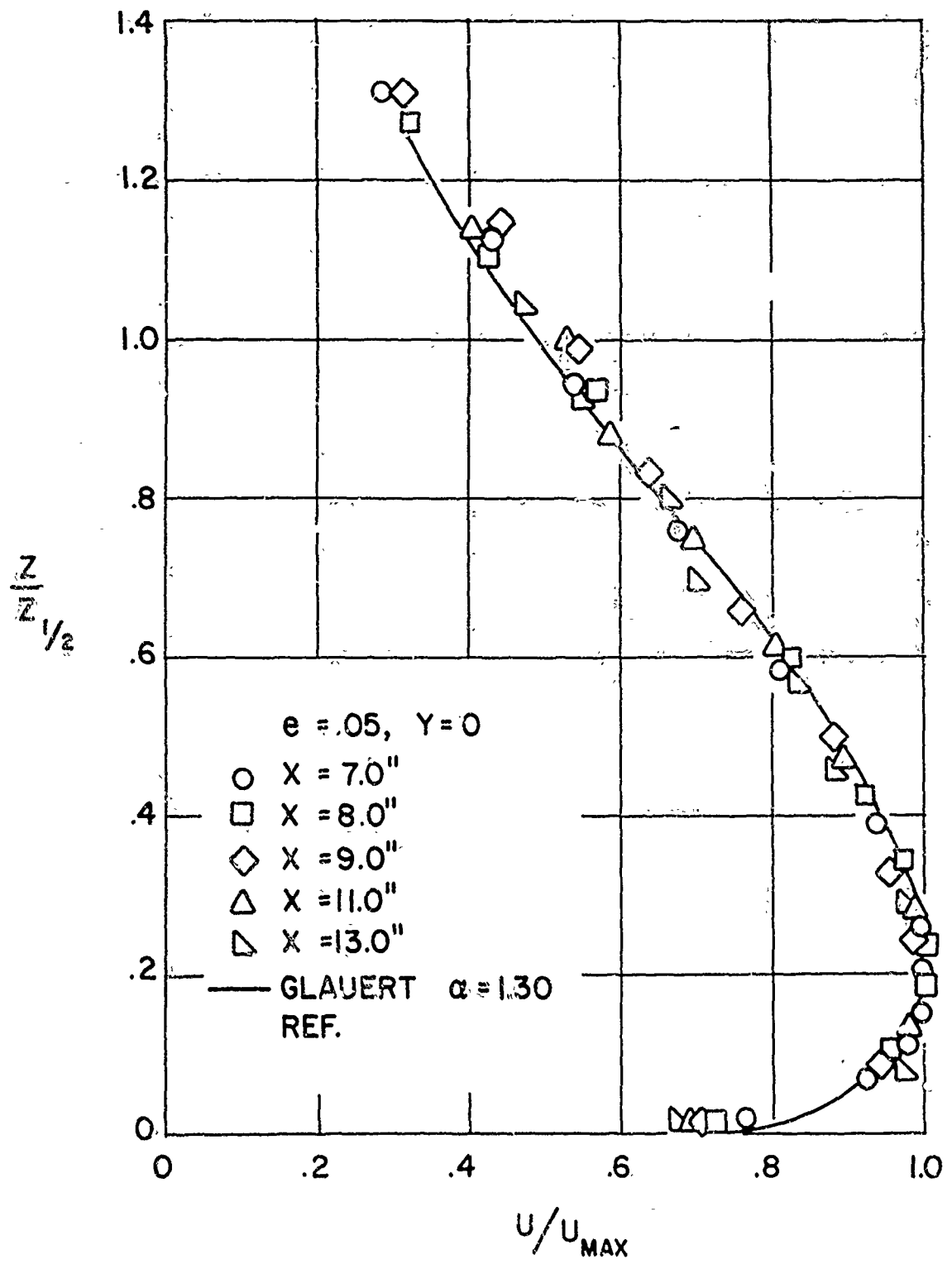


FIG.22 AXIAL VELOCITY PROFILES IN RADIAL TYPE DECAY REGION

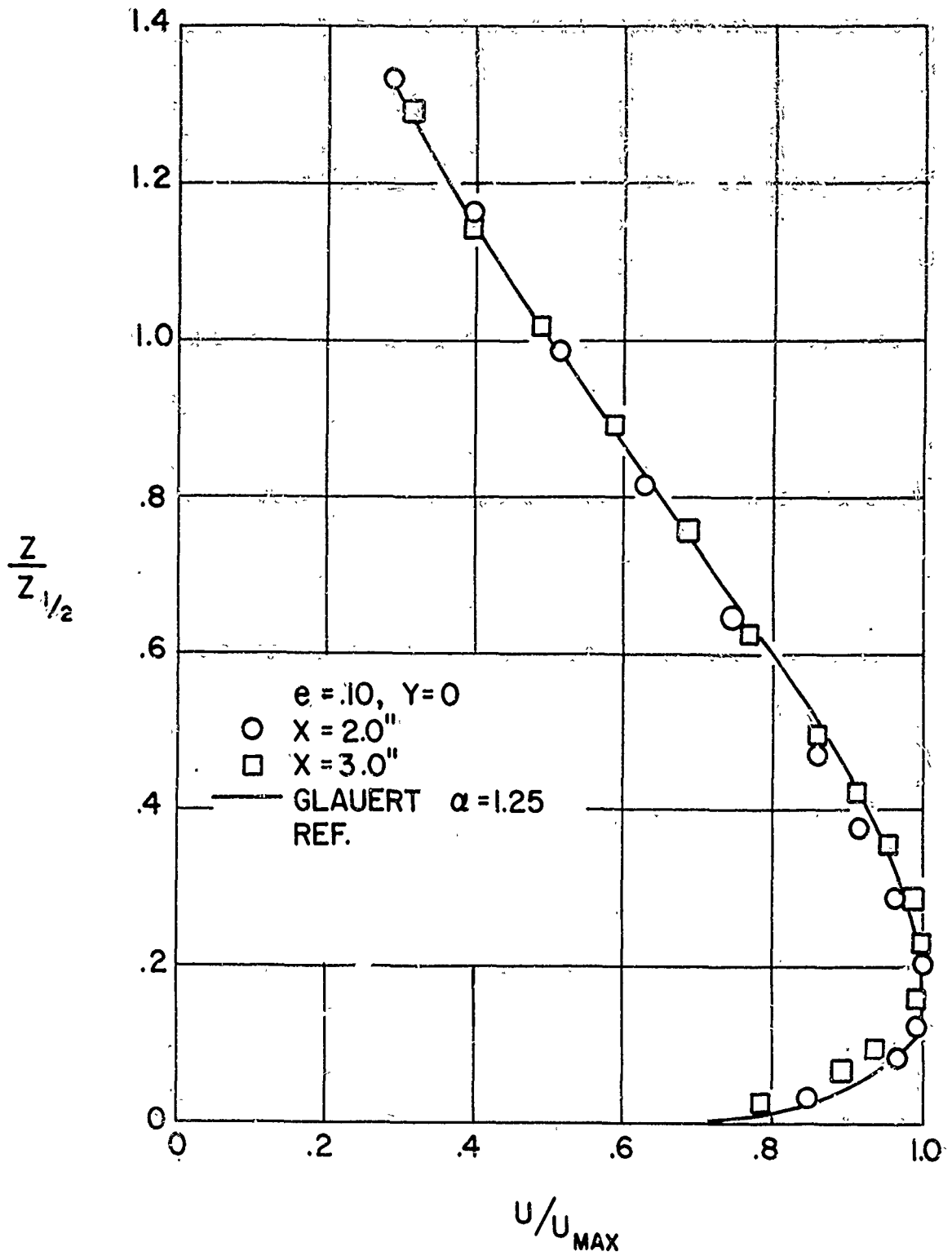


FIG. 23 AXIAL VELOCITY PROFILES IN CHARACTERISTIC DECAY REGION

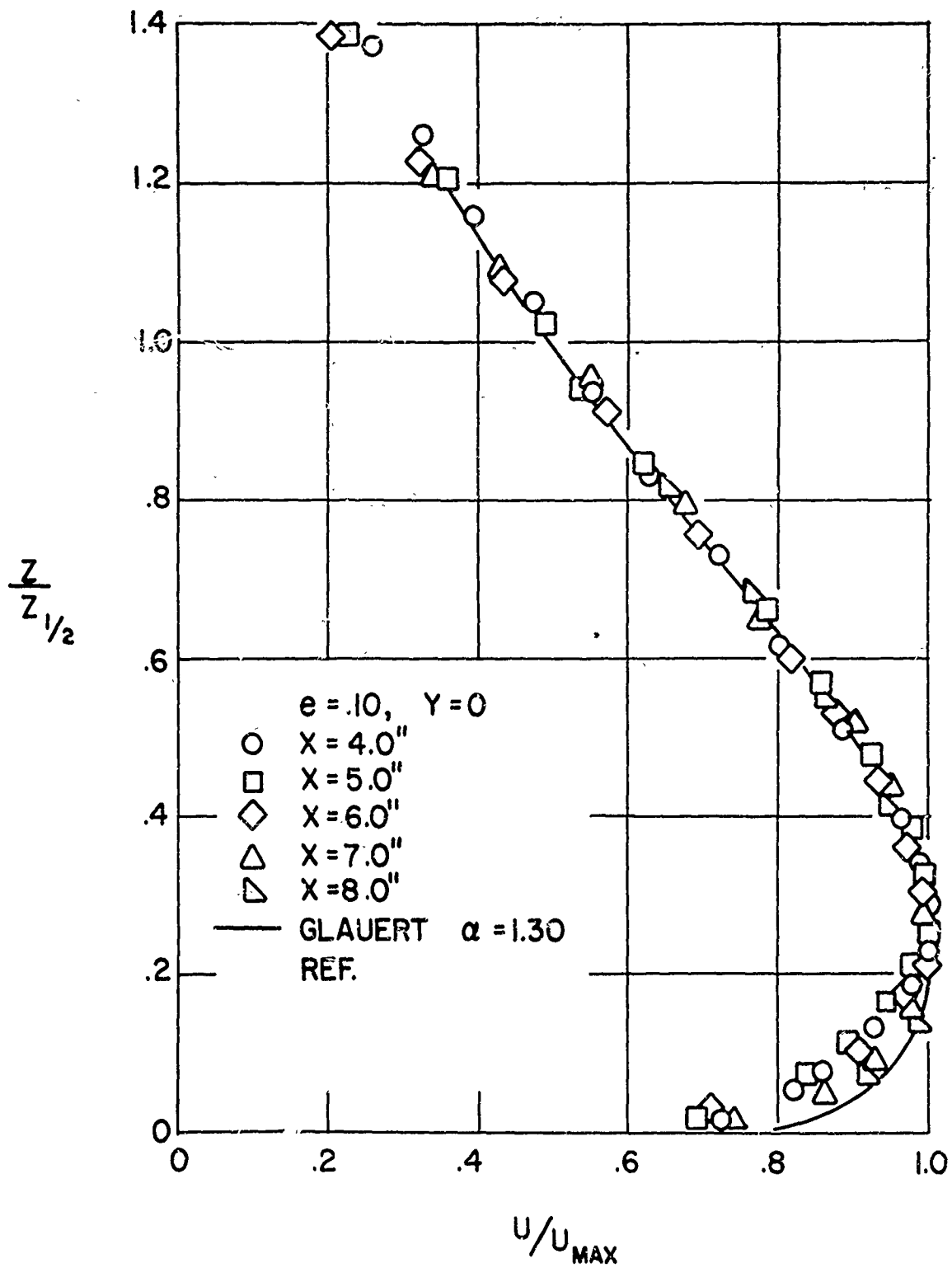


FIG.24 AXIAL VELOCITY PROFILES IN RADIAL TYPE DECAY REGION

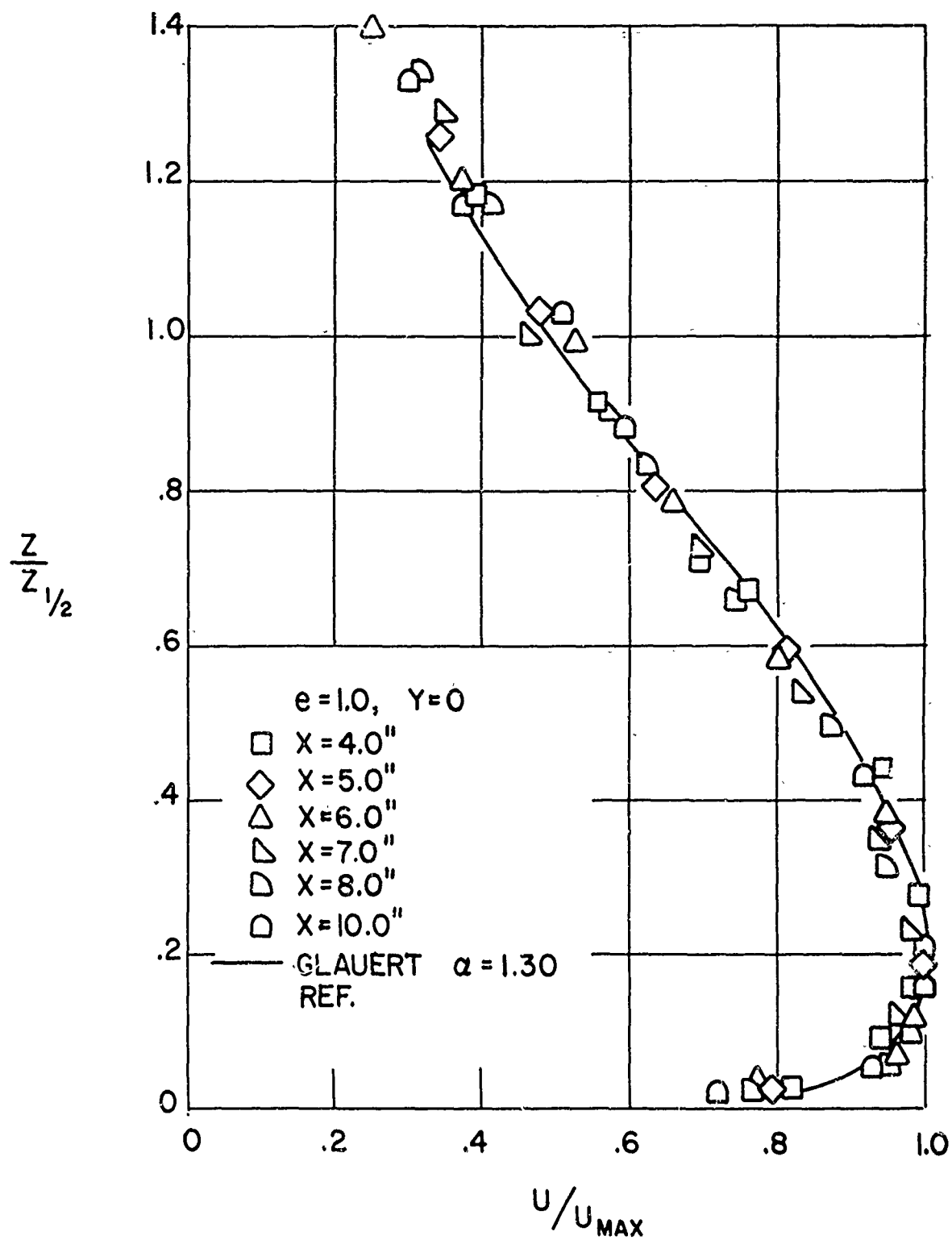


FIG.25 AXIAL VELOCITY PROFILES IN RADIAL TYPE DECAY REGION

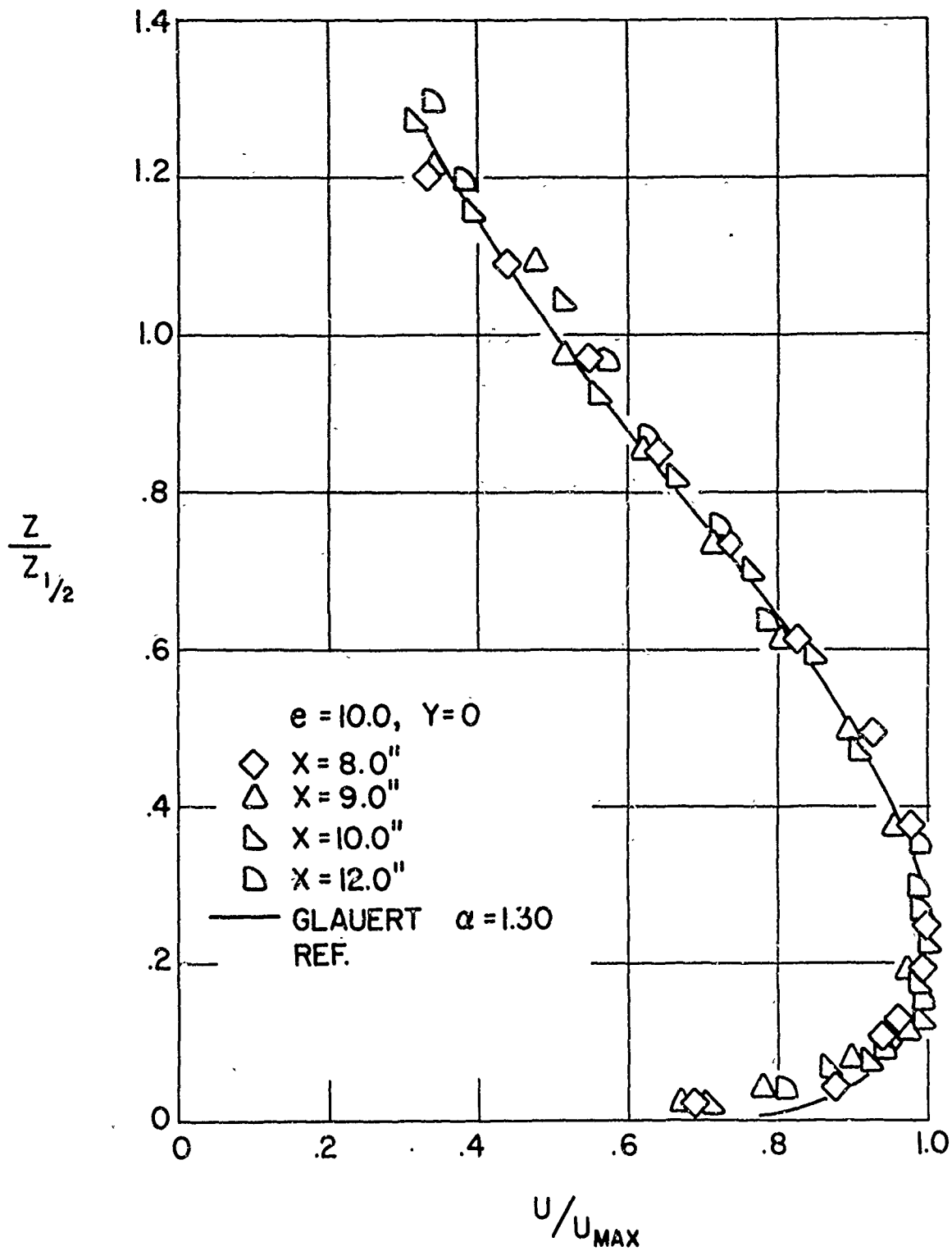


FIG. 26 AXIAL VELOCITY PROFILES IN RADIAL TYPE DECAY REGION

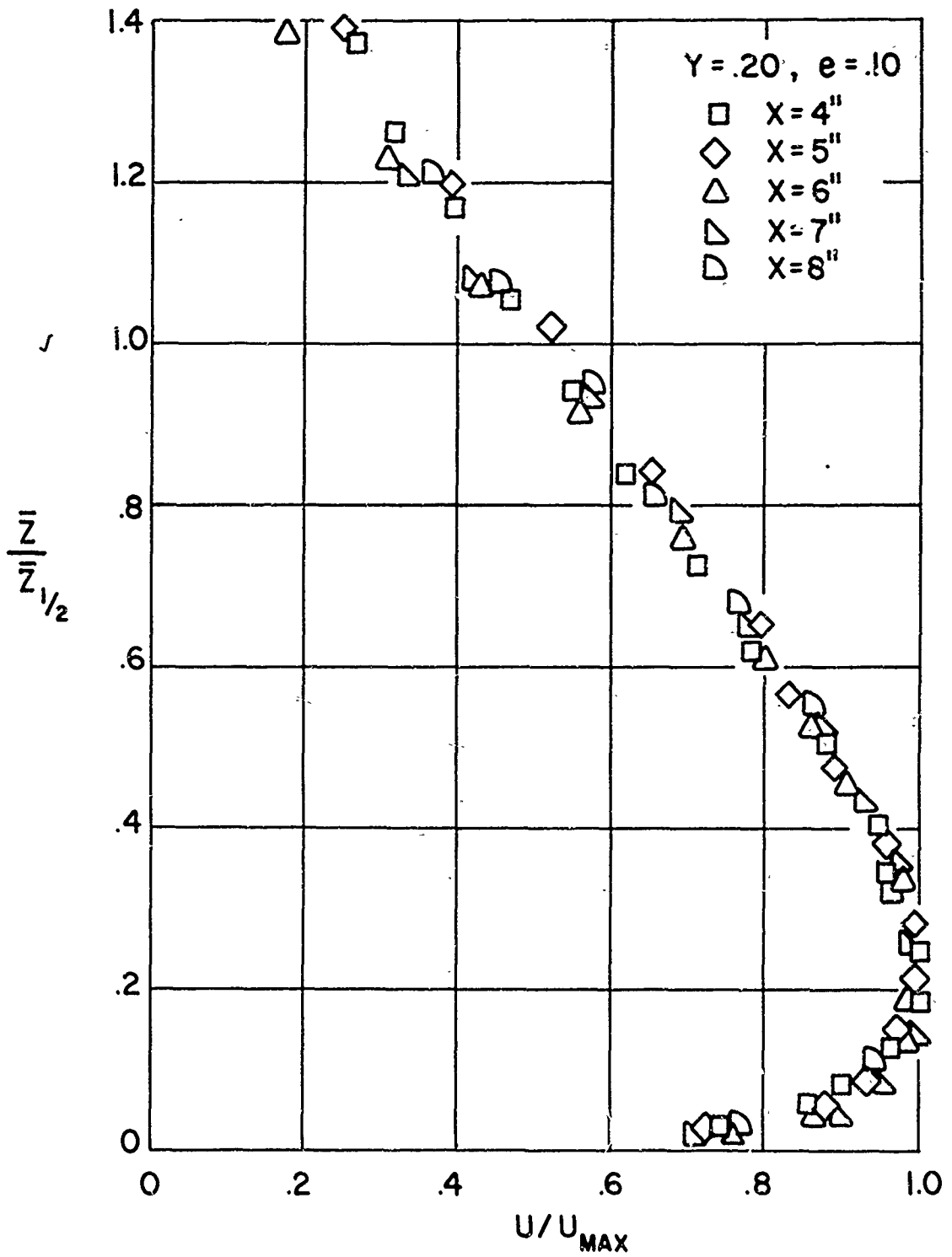


FIG. 27 AXIAL VELOCITY PROFILES IN RADIAL TYPE DECAY REGION

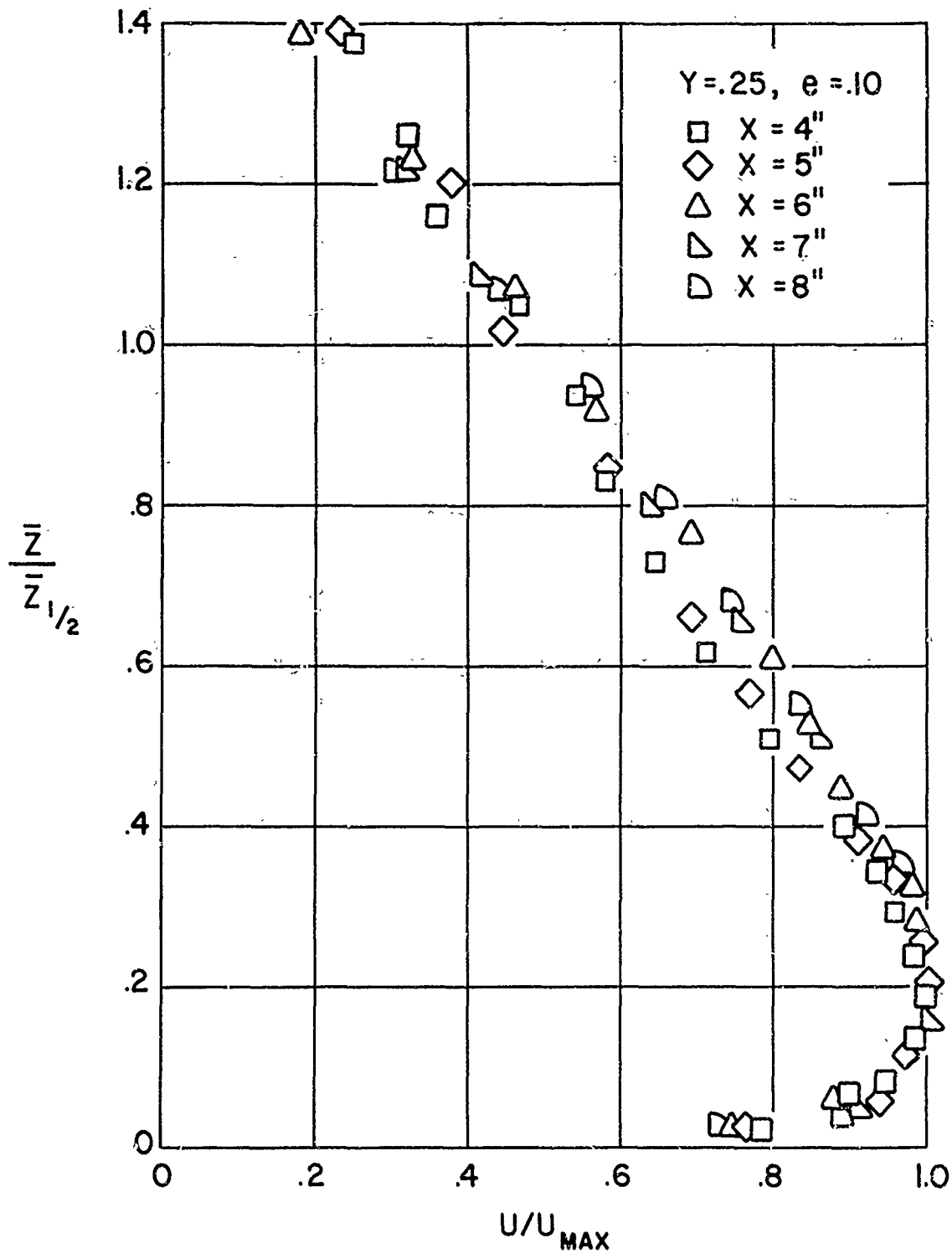


FIG. 28 AXIAL VELOCITY PROFILES IN RADIAL TYPE DECAY REGION

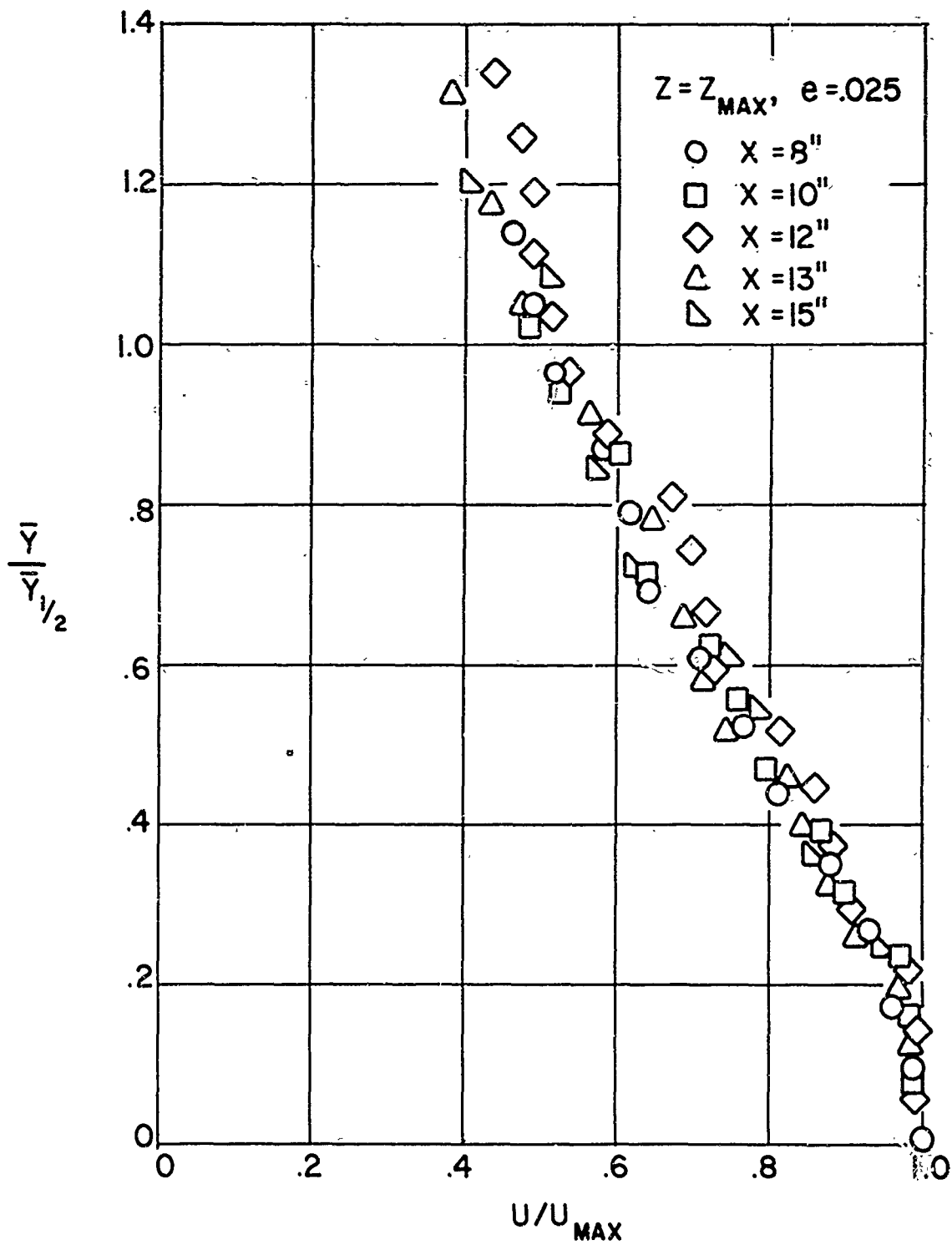


FIG. 29 TRANSVERSE VELOCITY PROFILES

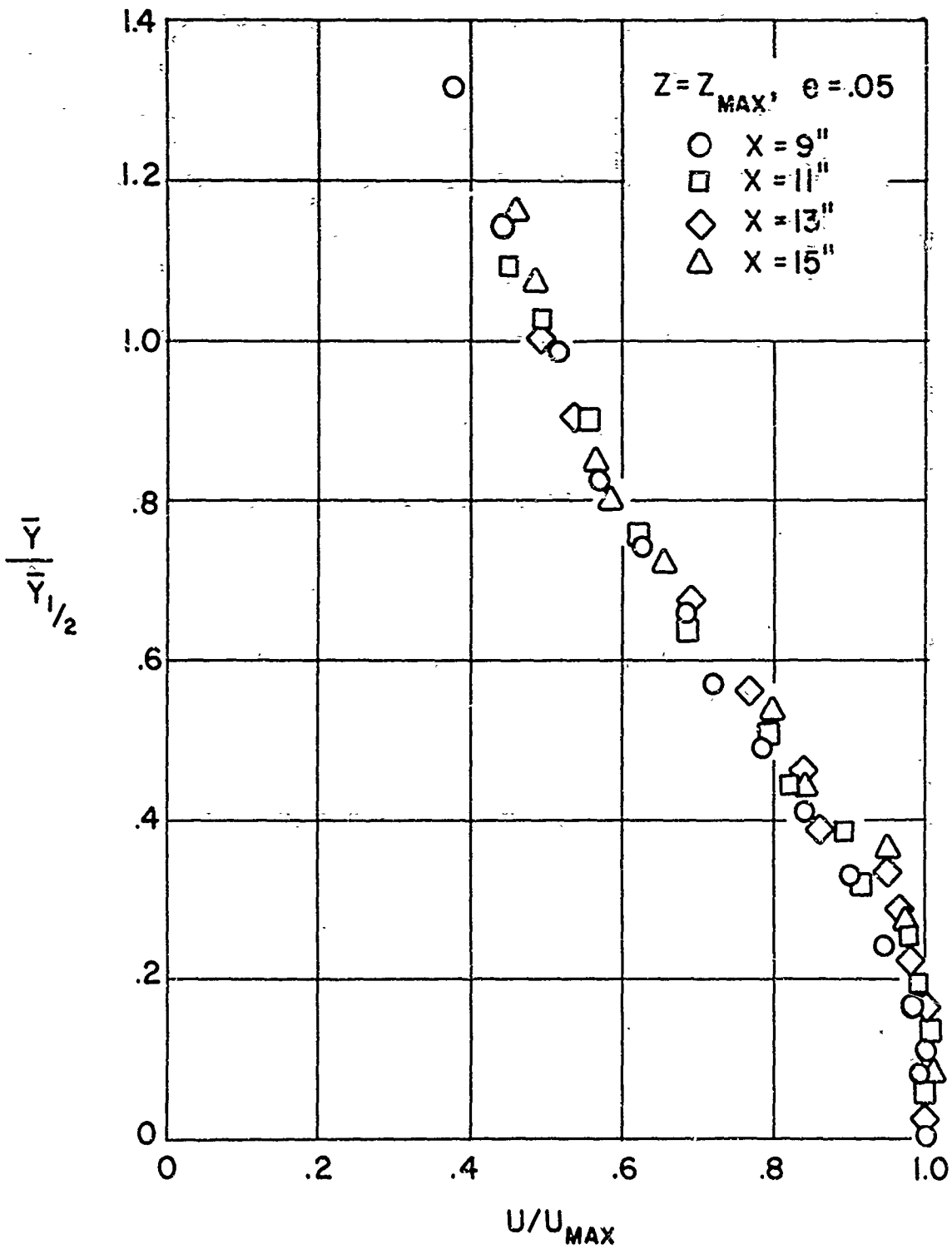


FIG. 30 TRANSVERSE VELOCITY PROFILES

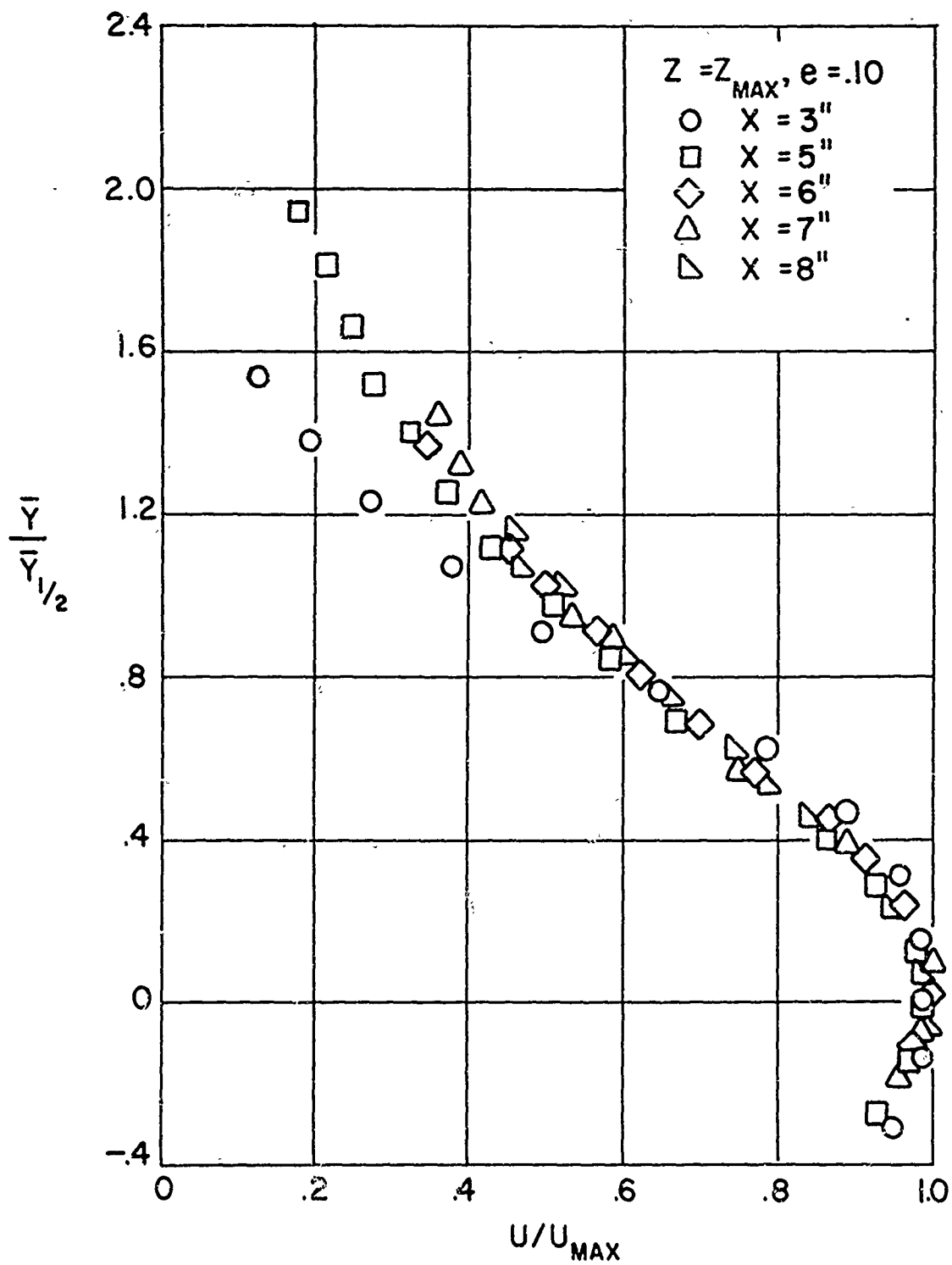


FIG. 32 TRANSVERSE VELOCITY PROFILES

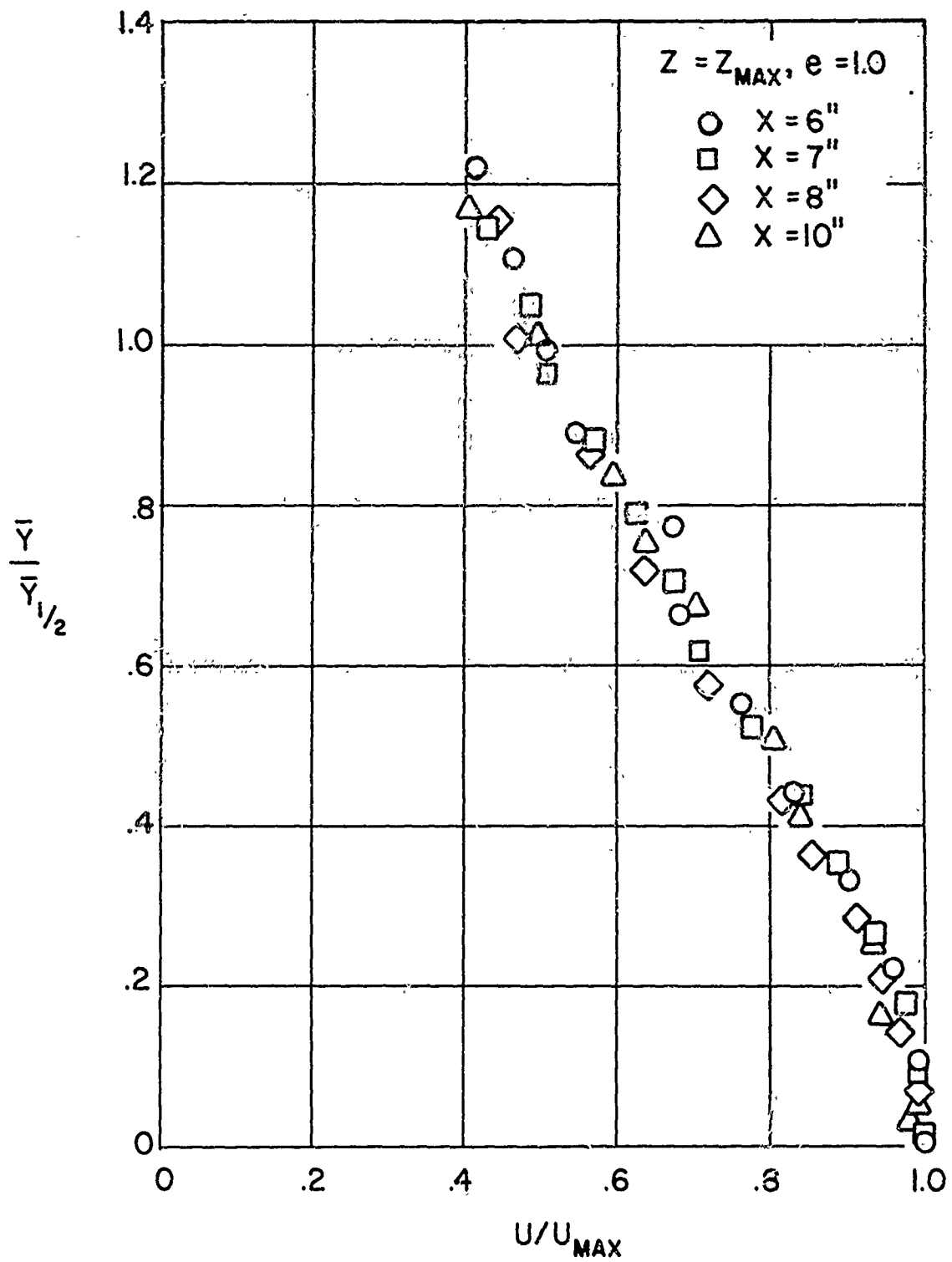


FIG. 33 TRANSVERSE VELOCITY PROFILES

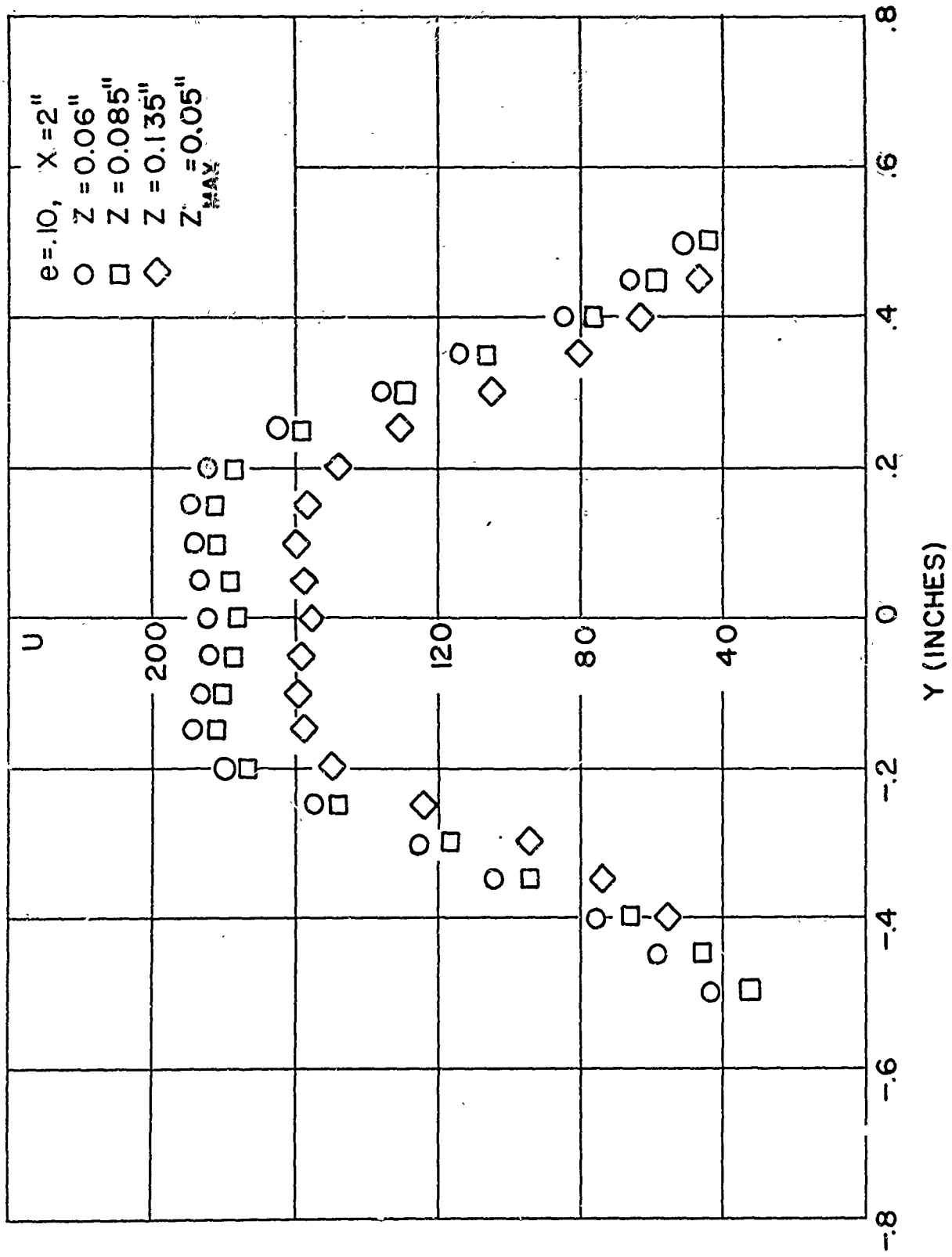


FIG. 34 TRANSVERSE VELOCITY PROFILES ($d = .10'$) FOR $e = .10$ SLOT

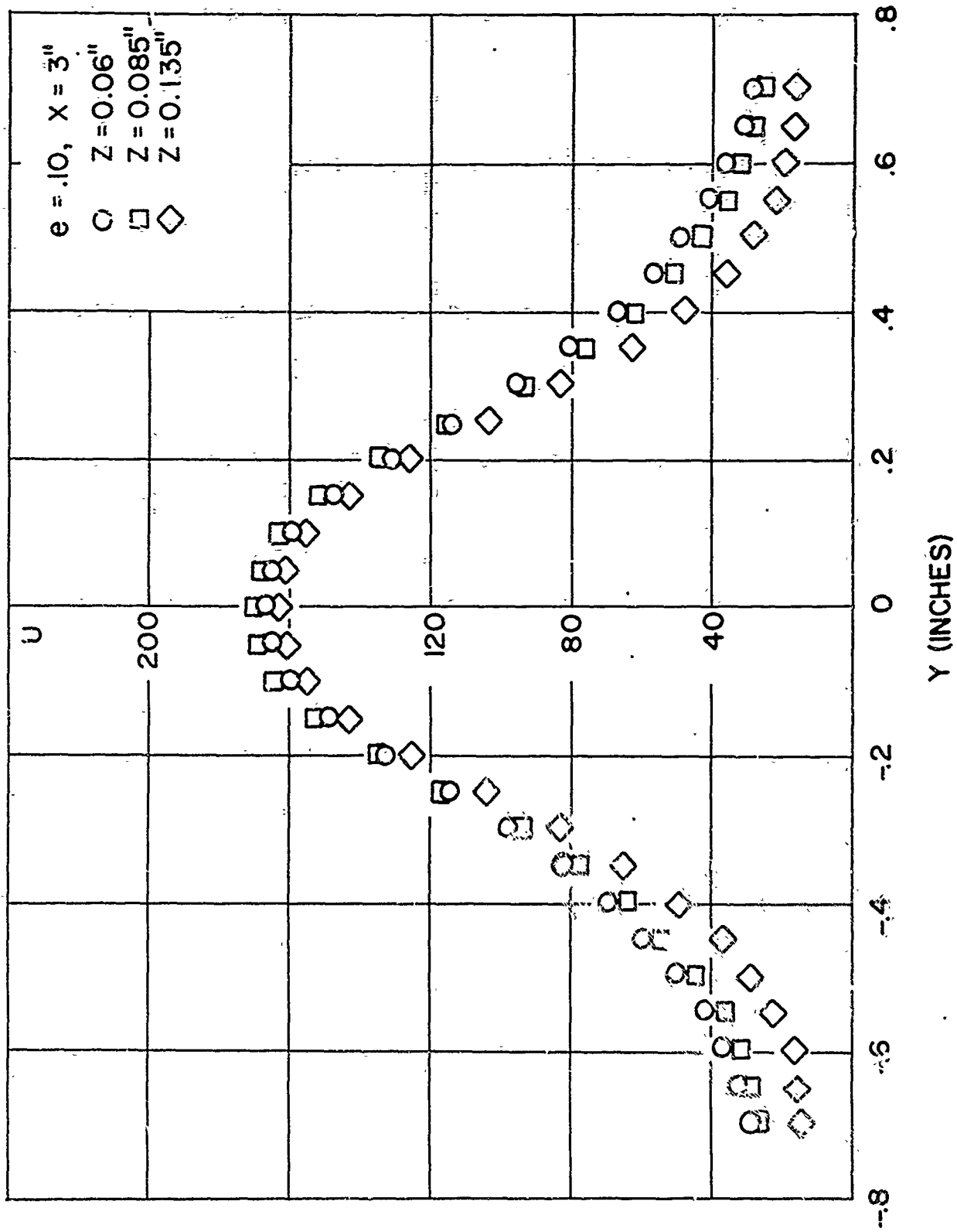


FIG. 35 TRANSVERSE VELOCITY PROFILES ($d = .10'$) FOR $e = .10$ SLOT

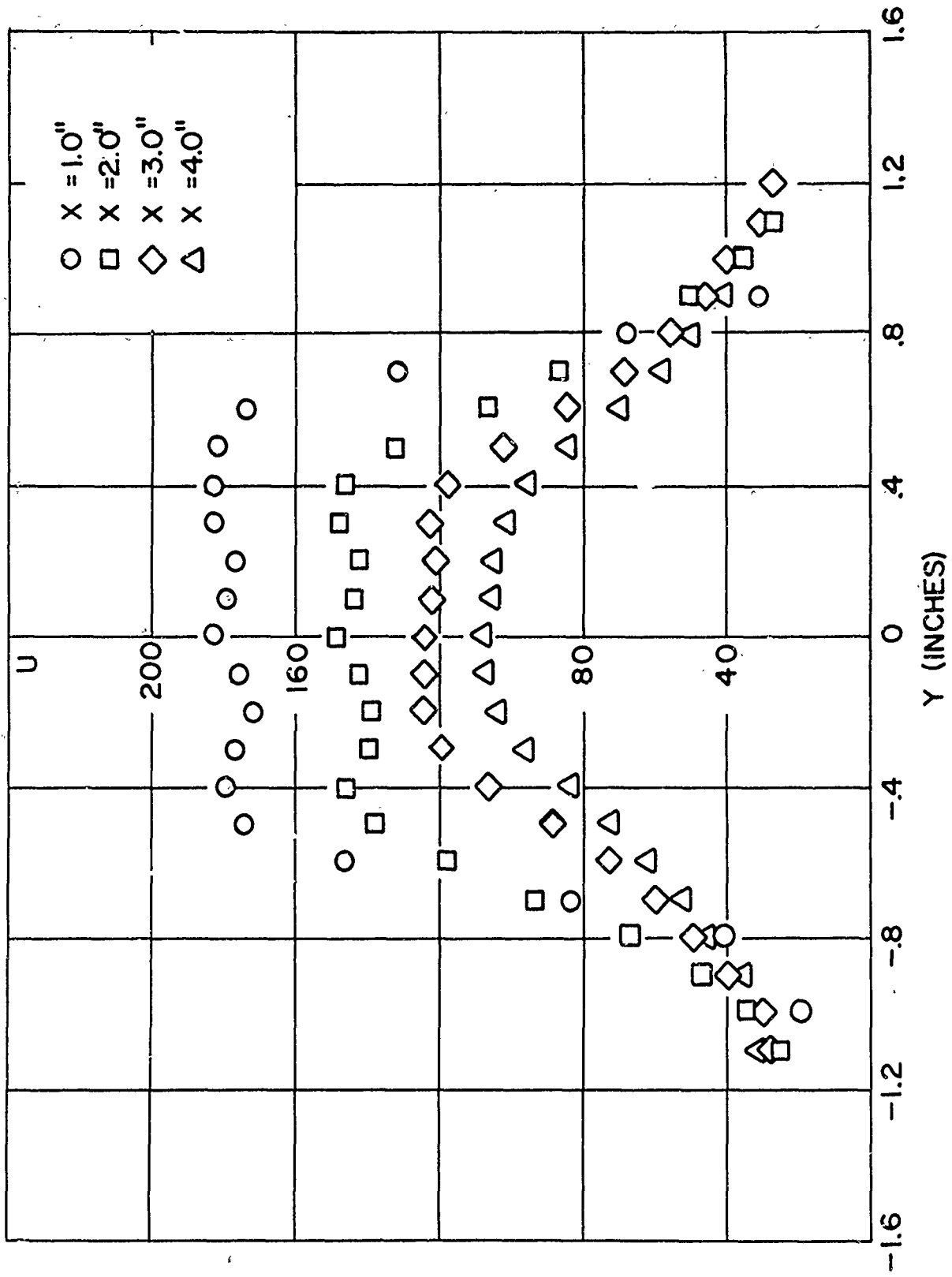


FIG. 36 TRANSVERSE VELOCITY PROFILES ($d = 0.07$) FOR $e = 0.05$
SLOT

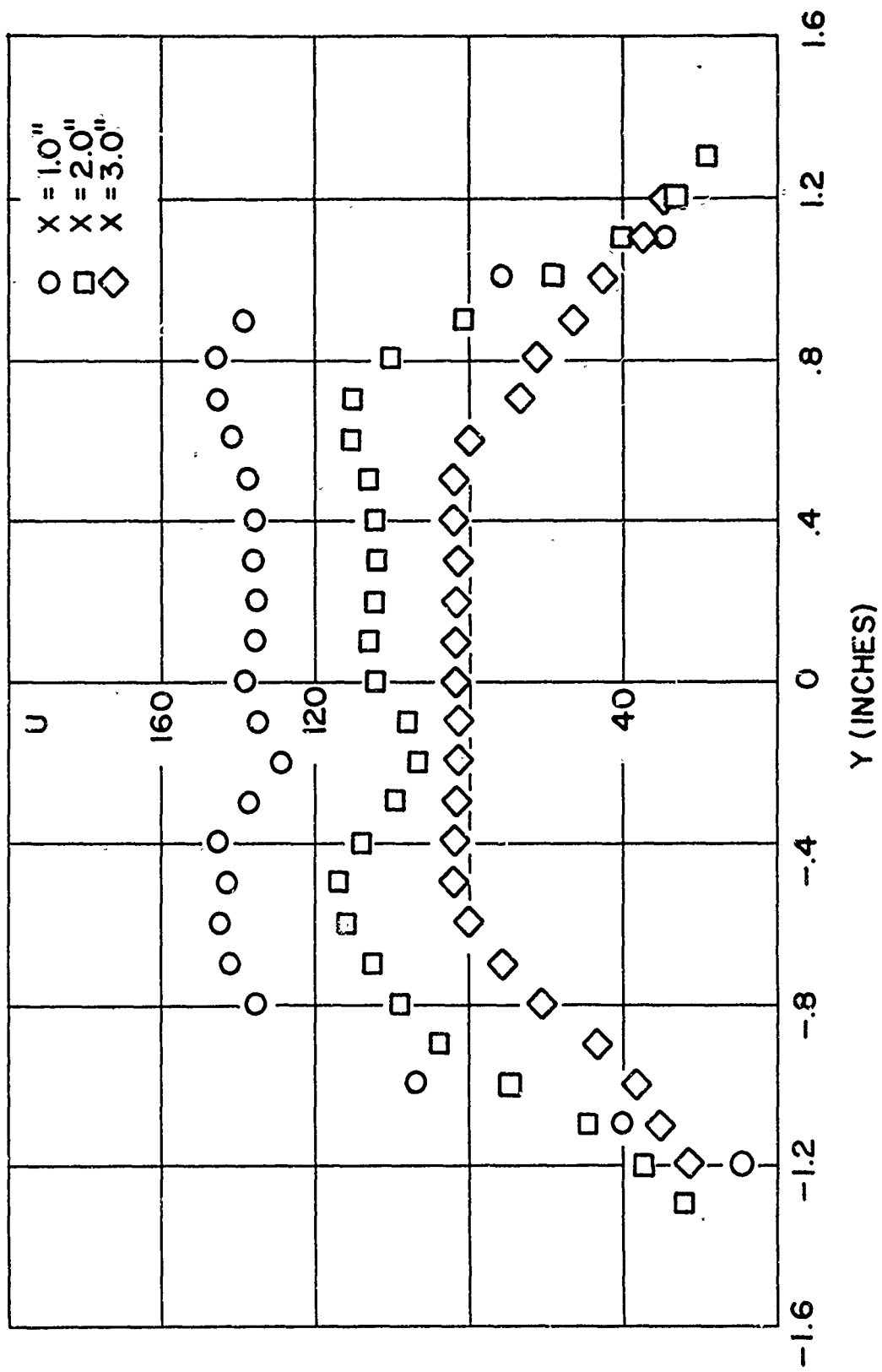


FIG. 37 TRANSVERSE VELOCITY PROFILES ($d = .05''$) FOR $e = .025$
 SLOT

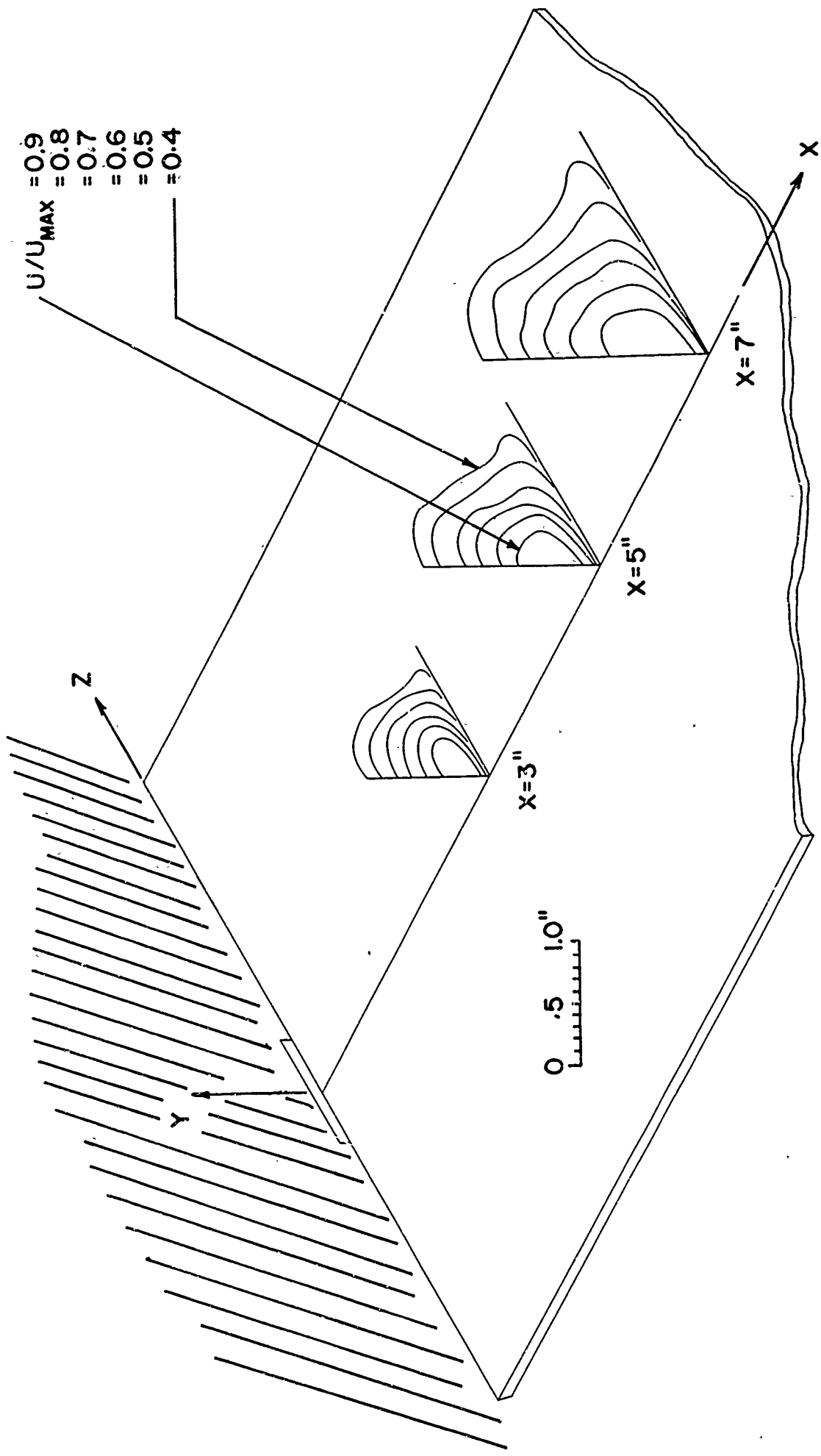


FIG. 38 CONTOURS OF CONSTANT VELOCITY FOR $e = 0.10$ SLOT

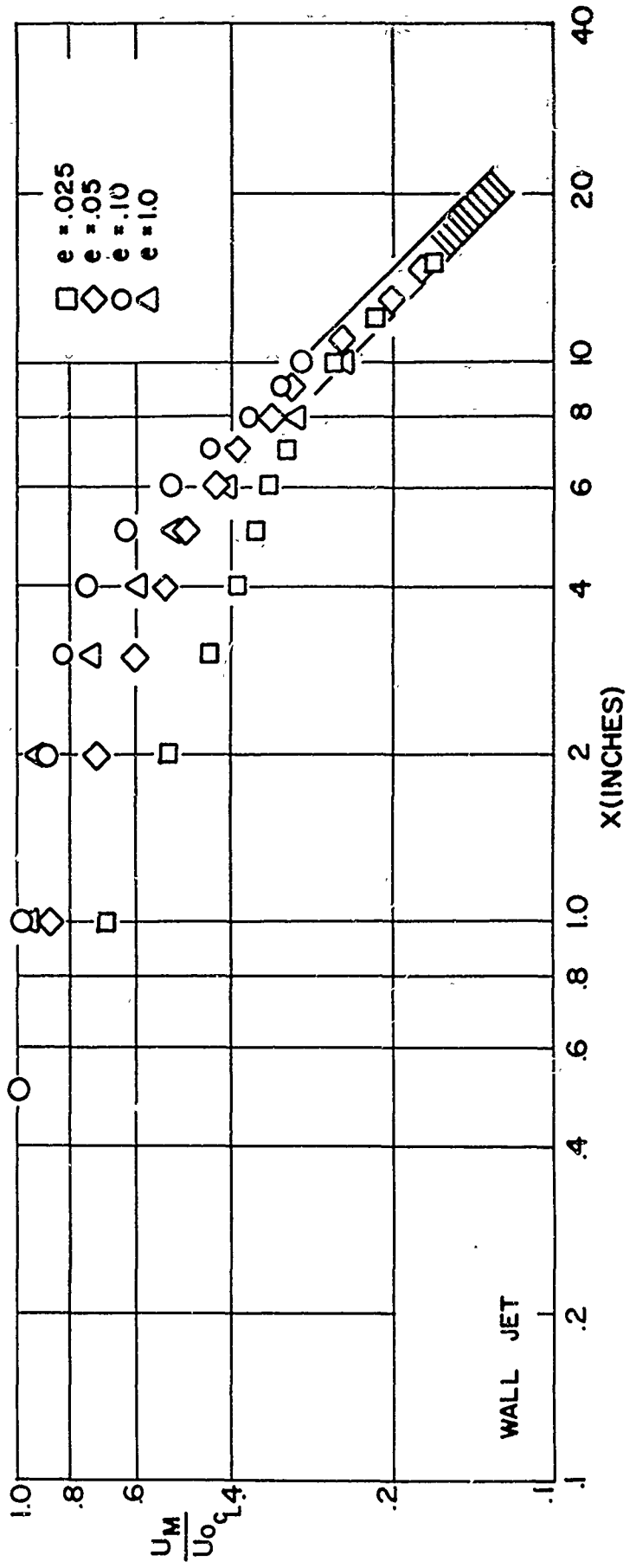
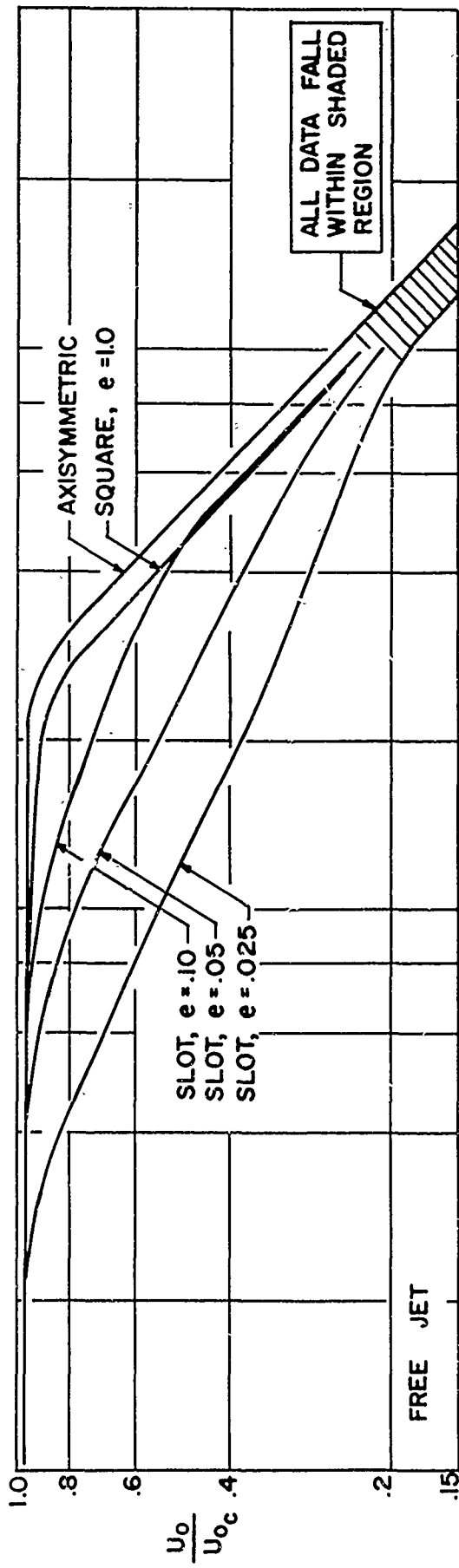


FIG. 39 COMPARISON OF MAXIMUM VELOCITY DECAY FOR FREE JET AND WALL JET

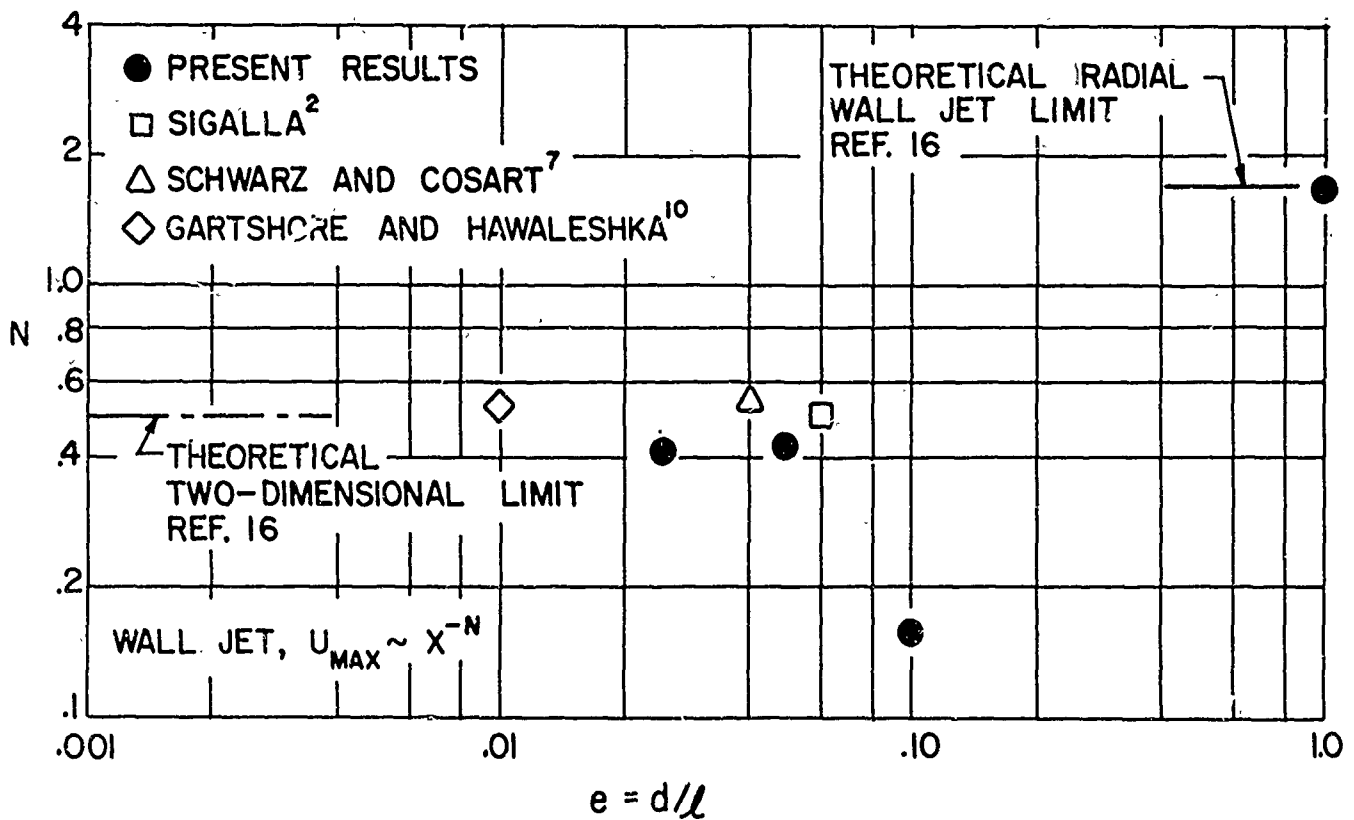
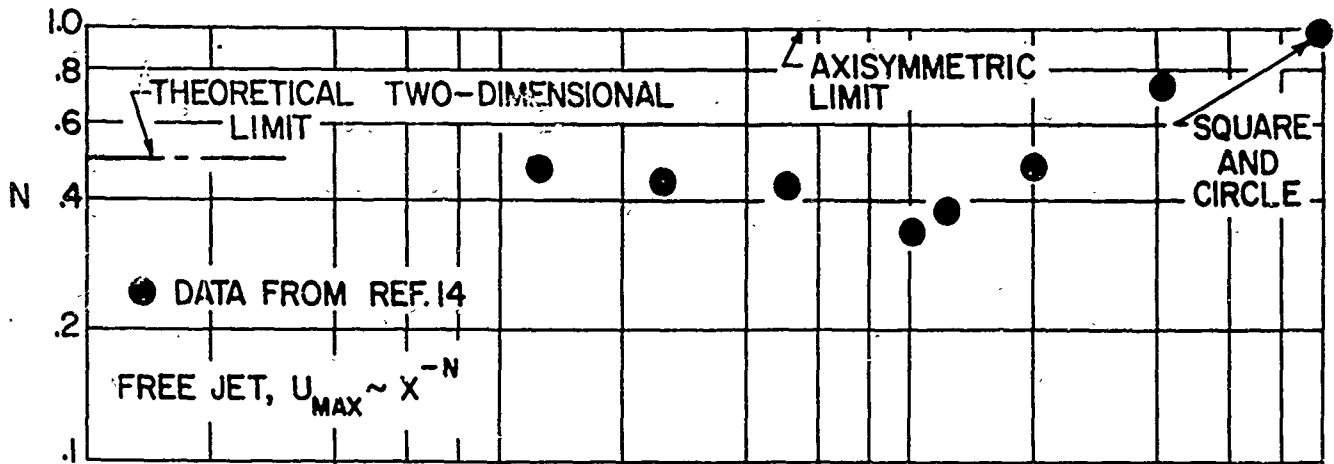


FIG. 40 EXPONENT (N) OF MAXIMUM VELOCITY DECAY FOR FREE JETS AND WALL JETS WITHIN CD REGION

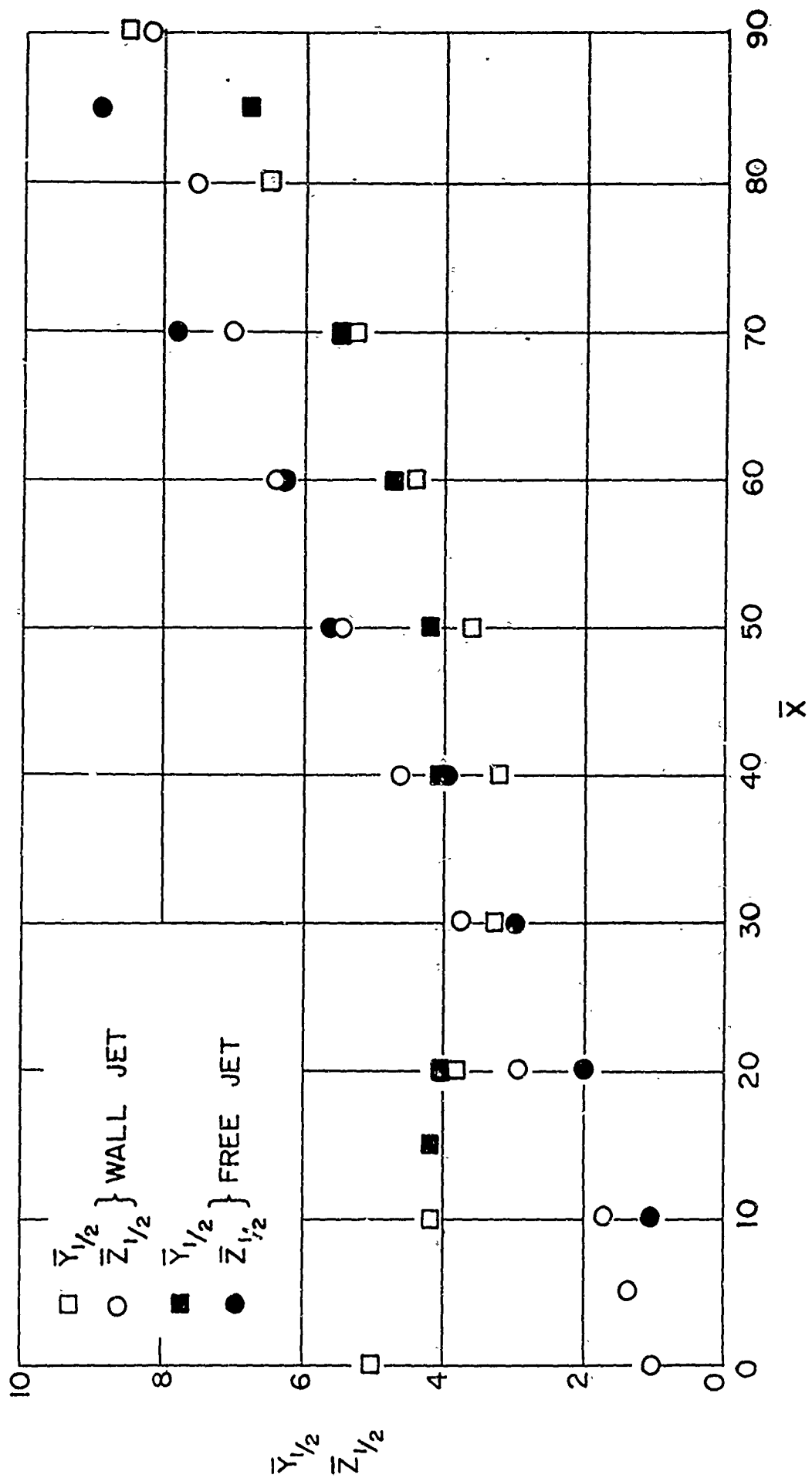


FIG. 41 COMPARISON OF FREE JET AND WALL JET FOR $e = .10$

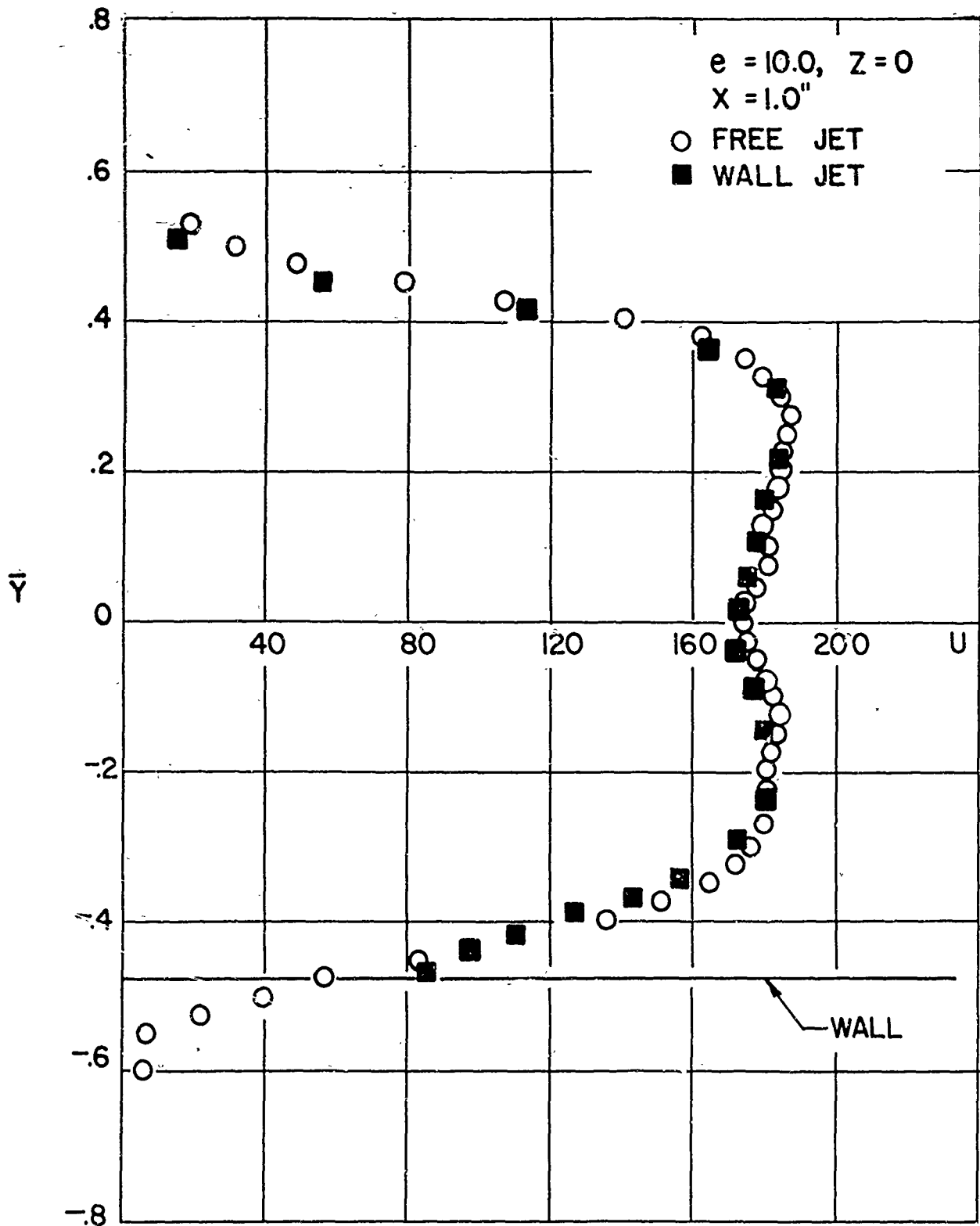


FIG. 42 COMPARISON OF MEAN VELOCITY PROFILES BETWEEN WALL JET AND FREE JET EMANATING FROM SAME ($e = 0.10$) ORIFICE, $X = 1.0$ INCH

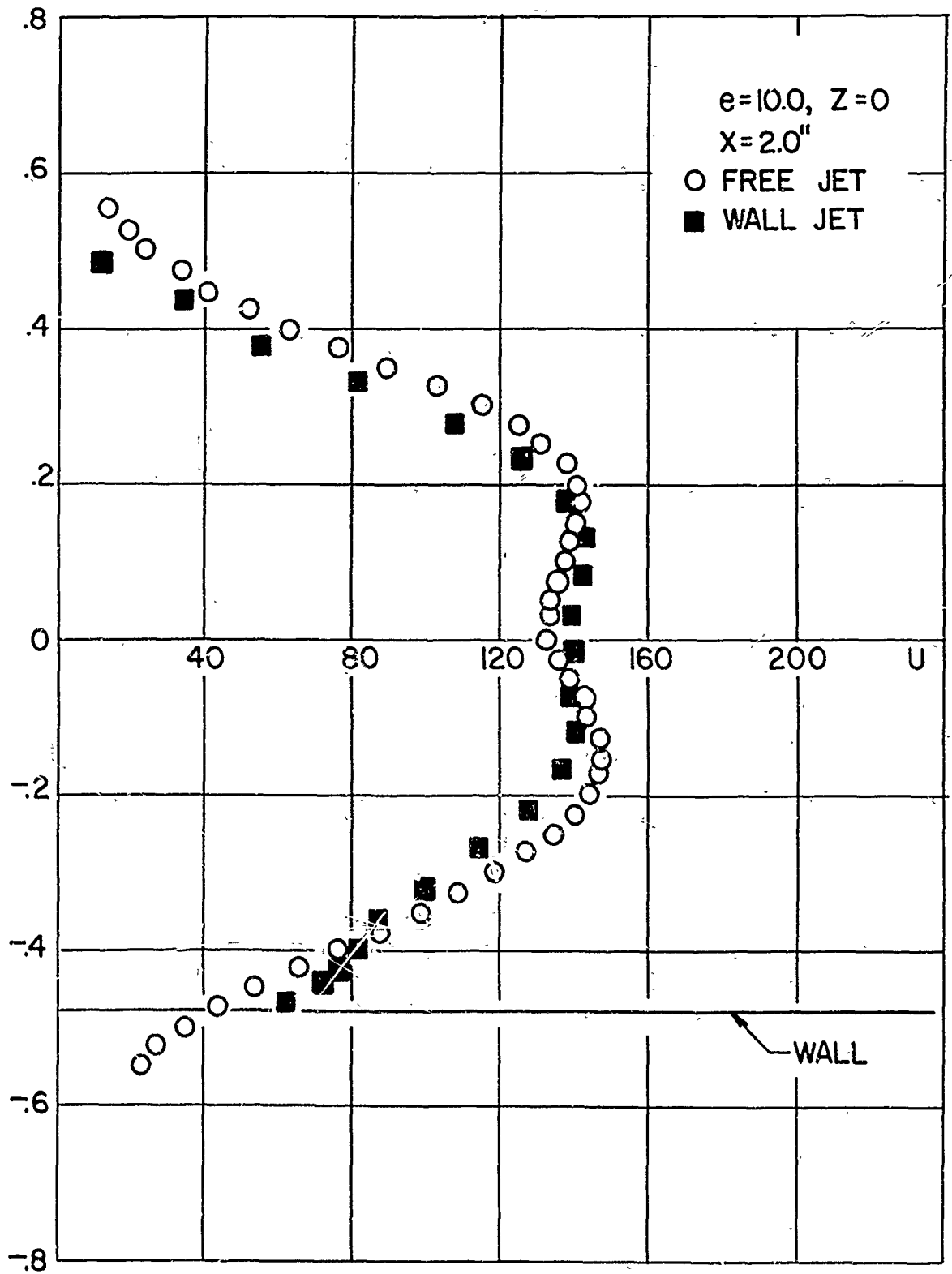
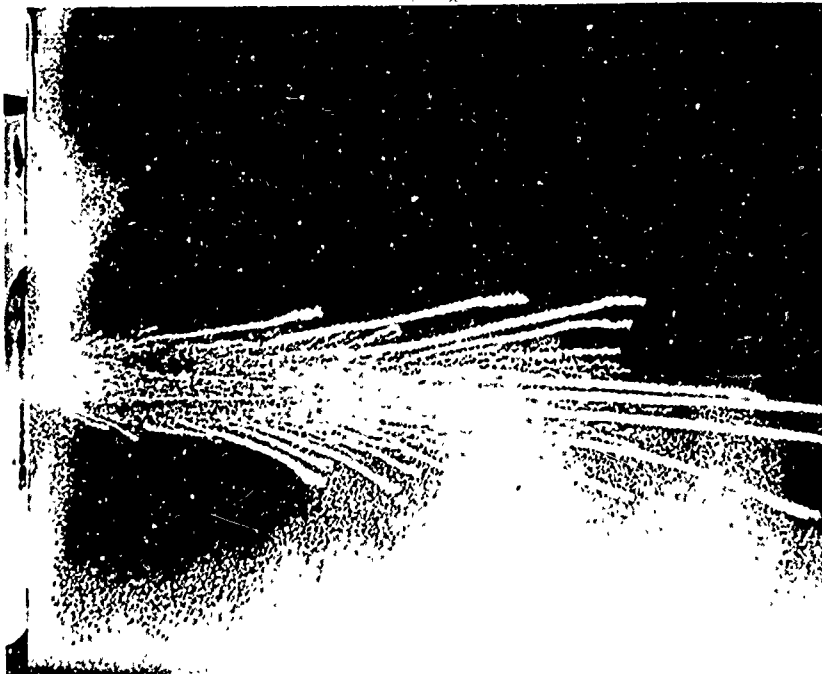


FIG. 43 COMPARISON OF MEAN VELOCITY PROFILES BETWEEN WALL JET AND FREE JET EMANATING FROM SAME ($e=0.10$) ORIFICE, $X=2.0$ INCH

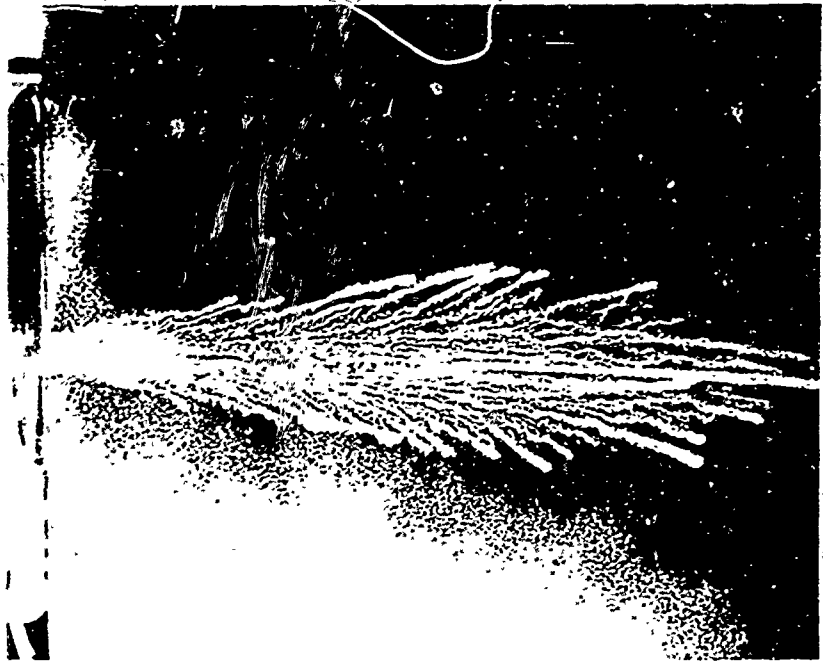


(a) $e=0.025$

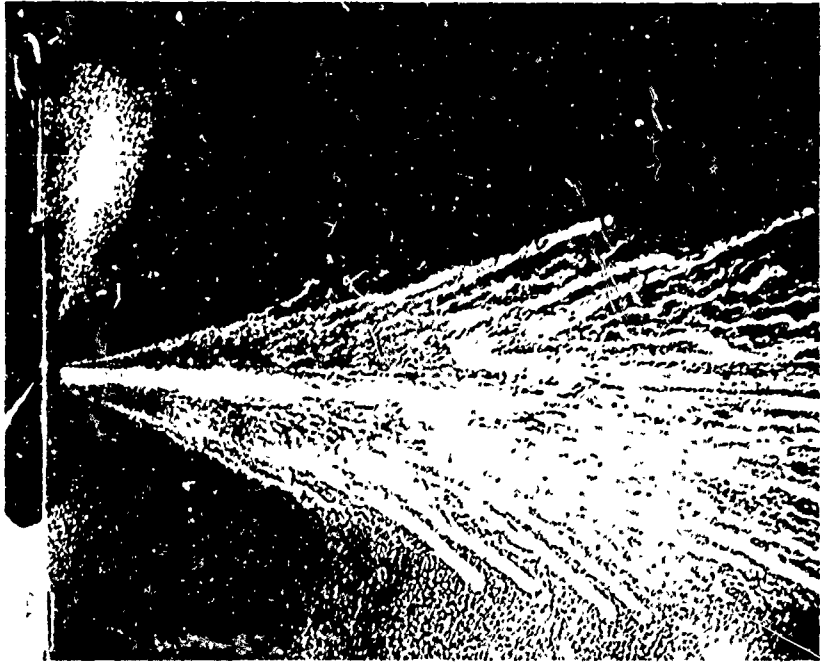


(b) $e=0.05$

FIG. 44 SURFACE FLOW STUDIES

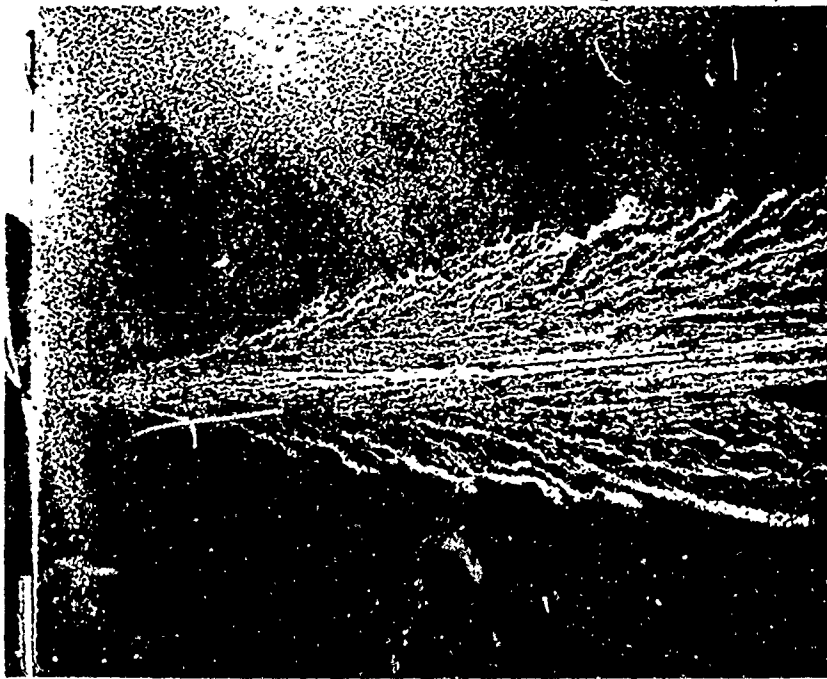


(c) $e = 0.10$



(d) $e = 1.0$

FIG. 44 SURFACE FLOW STUDIES (CONTINUED)



(e) $e = 10.0$

FIG. 44 SURFACE FLOW STUDIES (CONCLUDED)



(a)



(b)

FIG. 45 SIDE (a) AND TOP (b) VIEW OF
 $e = 0.05$ FLOW FIELD



(a)



(b)

FIG. 46 SIDE (a) AND TOP (b) VIEW OF
 $e = 1.0$ FLOW FIELD



(a) LAMINAR



(b) TURBULENT

FIG. 47 THREE-QUARTER VIEW OF $e = 0.10$
FLOW FIELD

Unclassified

Security Classification

DOCUMENT CONTROL DATA - R & D		
<i>(Security classification of title, body of abstract and indexing annotation must be entered when the overall report is classified.)</i>		
1. ORIGINATING ACTIVITY (Corporate author) Polytechnic Institute of Brooklyn Dept. of Aerospace Engrg. and Applied Mech. Route 110 Farmingdale, New York 11735		2a. REPORT SECURITY CLASSIFICATION Unclassified
3. REPORT TITLE A STUDY OF THREE-DIMENSIONAL, INCOMPRESSIBLE, TURBULENT WALL JETS		2b. GROUP
4. DESCRIPTIVE NOTES (Type of report and inclusive dates) Scientific Interim		
5. AUTHOR(S) (First name, middle initial, last name) Pasquale M. Sforza Gary Herbst		
6. REPORT DATE October 1967	7a. TOTAL NO. OF PAGES 83	7b. NO. OF REFS 20
8a. CONTRACT OR GRANT NO. AF 49(638)-1623	9a. ORIGINATOR'S REPORT NUMBER(S) PIBAL Report No. 1022	
b. PROJECT NO. 9781-01	9b. OTHER REPORT NO(S) (Any other numbers that may be assigned this report) AFOSR 67-2580	
c. 61445014		
d. 681307		
10. DISTRIBUTION STATEMENT Distribution of this document is unlimited.		
11. SUPPLEMENTARY NOTES TECH, OTHER	12. SPONSORING MILITARY ACTIVITY AF Office of Scientific Research (SREM) 1400 Wilson Blvd. Arlington, Virginia 22209	
13. ABSTRACT This report presents an experimental investigation of the mean properties of turbulent, three-dimensional, incompressible air jets issuing into a quiescent air ambient from various rectangular orifices parallel to, and at the surface of, a flat plate. An analytical approach to estimate the shear stress distribution at the plate is also presented. The flow field of a three-dimensional wall jet is found to be characterized by three distinct regions in the axis velocity decay. From the results obtained it is concluded that for three-dimensional wall jets the maximum velocity in the flow in the near field exhibits a decay rate dependent on orifice geometry, while far downstream of the jet exit it decays at the same rate as that in a radial wall jet flow field independent of orifice geometry. Furthermore, it is shown that the growth of the mixing layer normal to the plate is apparently independent of orifice shape while the near field spanwise growth is affected by initial geometry. Irregularities in the spanwise distribution of streamwise mean velocity attest to the strong three-dimensionality in the near field of the wall jets studied. These irregularities are manifested as local excesses or defects, in the velocity profile. Such results indicate that the characterization of the wall jet flow field generated by a finite slot as quasi-two-dimensional may be of questionable validity.		

DD FORM 1 NOV 65 1473

Unclassified

Security Classification

14	KEY WORDS	LINK A		LINK B		LINK C	
		ROLE	WT	ROLE	WT	ROLE	WT
	Three-dimensional Turbulent Incompressible Wall jets						